

ANALYSIS OF PARALLEL SCHWARZ ALGORITHMS FOR TIME-HARMONIC PROBLEMS USING BLOCK TOEPLITZ MATRICES*

N. BOOTLAND[†], V. DOLEAN[‡], A. KYRIAKIS[†], AND J. PESTANA[†]

Abstract. In this work we study the convergence properties of the one-level parallel Schwarz method applied to the one-dimensional and two-dimensional Helmholtz and Maxwell's equations. One-level methods are not scalable in general. However, it has recently been proven that when impedance transmission conditions are used in the case of the algorithm applied to the equations with absorption, under certain assumptions, scalability can be achieved and no coarse space is required. We show here that this result is also true for the iterative version of the method at the continuous level for strip-wise decompositions into subdomains that can typically be encountered when solving wave-guide problems. The convergence proof relies on the particular block Toeplitz structure of the global iteration matrix. Although non-Hermitian, we prove that its limiting spectrum has a near identical form to that of a Hermitian matrix of the same structure. We illustrate our results with numerical experiments.

Key words. domain decomposition methods, Helmholtz equations, Maxwell equations, Schwarz algorithms, one-level methods, block Toeplitz matrices

AMS subject classifications. 65N55, 65N35, 65F10, 15A18, 15B05

1. Introduction. Time-harmonic wave propagation problems, such as those arising in electromagnetic and seismic applications, are notoriously difficult to solve for several reasons. At the continuous level, the underlying boundary value problems lead to non self-adjoint operators (when impedance boundary conditions are used). The discretisation of these operators by a Galerkin method requires an increasing number of discretisation points as the wave number gets larger in order to avoid the pollution effect, meaning a shift in the numerical wave velocity with respect to the continuous one [1]. This leads to increasingly large linear systems with non-Hermitian matrices that are difficult to solve by classical iterative methods [13].

In the past two decades, different classes of efficient solvers and preconditioners have been devised; see the review paper [15] and references therein. One important class is based on domain decomposition methods [8], which are a good compromise between direct and iterative methods. Some of these domain decomposition methods rely on improving the transmission conditions, that pass data between subdomains, to give optimised transmission conditions; see the seminal work on Helmholtz equations [14] and its extensions to Maxwell's equations [7, 6, 10, 12] as well as to elastic waves [3, 20]. For large-scale problems, in order to achieve robustness with respect to the number of subdomains (scalability) and the wave number, two-level domain decomposition solvers have been developed in recent years: they are based on the idea of using the absorptive counterpart of the equations as a preconditioner, which in turn is solved by a domain decomposition method. These methods were successfully applied to Helmholtz and Maxwell's equations, which arise naturally in different applications [2, 9, 17].

*The first two authors gratefully acknowledge support from the EPSRC grant EP/S004017/1. The fourth author gratefully acknowledges support from the EPSRC grant EP/R009821/1.

[†]Department of Mathematics and Statistics, University of Strathclyde, Glasgow, UK (niall.bootland@strath.ac.uk, alexandros.kyriakis@strath.ac.uk, jennifer.pestana@strath.ac.uk).

[‡]Department of Mathematics and Statistics, University of Strathclyde, Glasgow, UK and Laboratoire J.A. Dieudonné, CNRS, University Côte d'Azur, Nice, France (work@victoritadolean.com).

However, an alternative idea emerged in the last few years by observing that, when using Robin or impedance transmission conditions, under certain assumptions involving the physical and numerical parameters of the problem (i.e. absorption, size of the subdomains, etc.) one-level Schwarz algorithms can scale (behave independently of the number of subdomains) without the addition of a second level [16, 18]. We would like to explore this idea at the continuous level (independent of the discretisation) for a strip-wise decomposition into subdomains as it arises naturally in the solution of wave-guide problems. The main contributions of the paper are the following:

- We provide analysis of the limiting spectrum, as the number of subdomains grows, for a one-level Schwarz method applied to a strip-wise decomposition. While our analysis is limited to this simple yet realistic configuration, it is valid at the continuous level both for one-dimensional and two-dimensional Helmholtz and Maxwell's equations.
- We build on the formalism introduced in [4] for the iteration matrices at the interface but we are able to characterise the entire spectrum of these iteration matrices by using their block Toeplitz structure.
- Despite the fact that the block Toeplitz structure is non-Hermitian, and thus results from the standard literature do not apply in a straightforward manner, we prove that the limiting spectrum of the iteration matrices as their size grows (corresponding to an increasing number of subdomains) tends to the limit predicted by the eigenvalues of the symbol of the block Toeplitz matrix, except perhaps for two additional simple eigenvalues.
- We show that the limiting spectrum is descriptive of what is observed in practice numerically, even for a relatively small number of subdomains.

The structure of the paper is as follows: In [Section 2](#) we present our results on the limiting spectrum of a non-Hermitian block Toeplitz matrix whose characteristic polynomial verifies a three-term recurrence. In [Sections 3](#) and [4](#) we apply these results to the analysis of the iterative Schwarz algorithm in the one-dimensional and two-dimensional cases. We illustrate the theory with numerical results in [Section 5](#). Finally, [Section 6](#) draws together our conclusions.

2. A non-Hermitian block Toeplitz structure. Consider a non-Hermitian block Toeplitz matrix $\mathcal{T} \in \mathbb{C}^{2m \times 2m}$ of the form

$$(2.1a) \quad \mathcal{T} = \begin{bmatrix} A_0 & A_1 & & & \\ A_{-1} & A_0 & A_1 & & \\ & \ddots & \ddots & \ddots & \\ & & A_{-1} & A_0 & A_1 \\ & & & A_{-1} & A_0 \end{bmatrix},$$

where

$$(2.1b) \quad A_0 = \begin{bmatrix} 0 & b \\ b & 0 \end{bmatrix}, \quad A_1 = \begin{bmatrix} a & 0 \\ 0 & 0 \end{bmatrix}, \quad A_{-1} = \begin{bmatrix} 0 & 0 \\ 0 & a \end{bmatrix},$$

for some non-zero complex coefficients a and b . We will see in the sections that follow that such non-Hermitian block Toeplitz structures arise naturally for iterative Schwarz algorithms applied to wave propagation problems. We are interested in a characterisation of the complete spectrum of (2.1) when its dimension becomes large, equating to the many subdomain case for the Schwarz method.

The so-called Szegő formula enables the asymptotic spectrum, i.e. the spectrum as $m \rightarrow \infty$, of a wide class of Hermitian block Toeplitz matrices to be characterised by

the eigenvalues of an associated matrix-valued function called the (block) symbol [23]. For non-Hermitian matrices, analogous results do not exist in general [23], but do hold when the union of the essential ranges of the eigenvalues of the block symbol has empty interior and does not disconnect the complex plane [11]. Unfortunately, \mathcal{T} in (2.1) has symbol $F(z) = A_{-1}z + A_0 + A_1z^{-1}$ and, for relevant values of a and b , the union of essential ranges is a closed curve. Additional characterisations of the asymptotic spectrum of (block) banded Toeplitz matrices are available [19, 22, 26], but these do not provide explicit formulae for the eigenvalues, as we shall in Theorem 2.2. Other formulae for the eigenvalues [21] and determinant [24] of block tridiagonal Toeplitz matrices are known, however, they are applicable only when A_1 (or A_{-1}) is nonsingular. Accordingly, in this section we derive the limiting spectrum of \mathcal{T} .

In order to establish a result on the spectrum, we first show that the characteristic polynomials of (2.1) for increasing m obey a three-term recurrence relation.

LEMMA 2.1 (Three-term recurrence and generating function). *Let $p_m(z)$ denote the characteristic polynomial of the block Toeplitz matrix $\mathcal{T} \in \mathbb{C}^{2m \times 2m}$ defined in (2.1). Then $p_m(z)$ satisfies the three-term recurrence relation*

$$(2.2) \quad p_m(z) + B(z)p_{m-1}(z) + A(z)p_{m-2}(z) = 0, \quad \text{for } m \geq 2,$$

with $A(z) = a^2z^2$ and $B(z) = -z^2 + b^2 - a^2$ and where $p_0(z) = 1$ and $p_1(z) = z^2 - b^2$. Furthermore, this recurrence relation is encoded in the generating function

$$(2.3) \quad \sum_{m=0}^{\infty} p_m(z)t^m = \frac{N(t, z)}{D(t, z)},$$

where

$$(2.4a) \quad D(t, z) = 1 + B(z)t + A(z)t^2,$$

$$(2.4b) \quad N(t, z) = p_0(z) + (p_1(z) + B(z)p_0(z))t.$$

Thus, in our case, $D(t, z) = 1 - (z^2 - b^2 + a^2)t + a^2z^2t^2$ while $N(t, z) = 1 - a^2t$.

Proof. We first prove the recurrence relation. Let D_m be the $2m \times 2m$ matrix whose determinant is the characteristic polynomial of \mathcal{T} in the variable z . Note that the first two characteristic polynomials are

$$(2.5a) \quad p_1(z) = \det(D_1) = \begin{vmatrix} -z & b \\ b & -z \end{vmatrix} = z^2 - b^2,$$

$$(2.5b) \quad p_2(z) = \det(D_2) = \begin{vmatrix} -z & b & a & 0 \\ b & -z & 0 & 0 \\ 0 & 0 & -z & b \\ 0 & a & b & -z \end{vmatrix} = (z^2 - b^2)^2 - a^2b^2.$$

To derive a recurrence relation, let us also define the intermediary determinants

$$r_m(z) := \begin{vmatrix} b & a & 0 & 0 & \cdots \\ 0 & & & & \\ a & & & & \\ 0 & & & & \\ \vdots & & & & \end{vmatrix} D_{m-1} = \begin{vmatrix} b & a & 0 & 0 & \cdots \\ 0 & -z & b & a & 0 \\ a & b & -z & 0 & 0 \\ 0 & 0 & 0 & & \\ \vdots & 0 & a & & \end{vmatrix} D_{m-2} = b p_{m-1}(z) + a^2 r_{m-1}(z),$$

so that

$$p_m(z) = z^2 p_{m-1}(z) - b r_m(z) = (z^2 - b^2) p_{m-1}(z) - a^2 b r_{m-1}(z).$$

We can then rearrange this relation to give an expression for $r_{m-1}(z)$ in terms of $p_m(z)$ and $p_{m-1}(z)$. Substituting this into the recurrence for $r_m(z)$ above, along with the equivalent expression for $r_m(z)$, yields the desired recurrence relation

$$(2.6) \quad p_{m+1}(z) = (z^2 - b^2 + a^2) p_m(z) - a^2 z^2 p_{m-1}(z),$$

where $A(z) := a^2 z^2$ and $B(z) := -z^2 + b^2 - a^2$. Finally, note that setting $p_0 = 1$ is consistent with this recurrence relation and initial characteristic polynomials (2.5).

To show the equivalence of the generating function, we multiply (2.2) by t^m and sum over $m \geq 2$ before adding relevant terms to isolate $\sum_{m=0}^{\infty} p_m(z) t^m$ as follows

$$\begin{aligned} & \sum_{m=2}^{\infty} [p_m(z) + B(z)p_{m-1}(z) + A(z)p_{m-2}(z)] t^m = 0 \\ \iff & \sum_{m=0}^{\infty} [1 + B(z)t + A(z)t^2] p_m(z) t^m = p_0(z) + (p_1(z) + B(z)p_0(z)) t \\ \iff & \sum_{m=0}^{\infty} p_m(z) t^m = \frac{p_0(z) + (p_1(z) + B(z)p_0(z)) t}{1 + B(z)t + A(z)t^2}. \end{aligned}$$

Substituting in the appropriate values gives $D(t, z) = 1 - (z^2 - b^2 + a^2)t + a^2 z^2 t^2$ and $N(t, z) = 1 - a^2 t$ in our case, as required. \square

We now introduce a useful tool that will help us to characterise the spectrum of (2.1): the q -analogue of the discriminant known as the q -discriminant [25]. The q -discriminant of a polynomial $P_n(t)$ of degree n with leading coefficient p is defined as

$$(2.7) \quad \text{Disc}_t(P_n; q) = p^{2n-2} q^{n(n-1)/2} \prod_{1 \leq i < j \leq n} (q^{-1/2} t_i - q^{1/2} t_j)(q^{1/2} t_i - q^{-1/2} t_j),$$

where t_i , $1 \leq i \leq n$, are the roots of $P_n(t)$. A key point is that the q -discriminant is zero if and only if a quotient of roots t_i/t_j equals q . Note that as $q \rightarrow 1$ the q -discriminant becomes the standard discriminant of a polynomial.

In particular, we will consider the q -discriminant of the denominator $D(t, z)$ as a quadratic in t . Direct calculation using the quadratic formula yields

$$(2.8) \quad \text{Disc}_t(D(t, z); q) = q (B(z)^2 - (q + q^{-1} + 2)A(z)),$$

for any $q \neq 0$. If q is a quotient of the two roots in t of $D(t, z)$ then (2.8) is zero and so q must satisfy

$$(2.9) \quad \frac{B(z)^2}{A(z)} = q + q^{-1} + 2,$$

where, in general, q will depend on z . We now state our main result on the limiting spectrum of \mathcal{T} as its dimension becomes large in which we adapt some ideas from [25] for finding roots of polynomials verifying a three-term recurrence but now with a different generating function.

THEOREM 2.2 (Limiting spectrum). *The limiting spectrum, as $m \rightarrow \infty$, of the block Toeplitz matrix $\mathcal{T} \in \mathbb{C}^{2m \times 2m}$, defined in (2.1), lies on the curve defined by*

$$(2.10) \quad \lambda_{\pm}(\theta) = a \cos(\theta) \pm \sqrt{b^2 - a^2 \sin^2(\theta)}, \quad \theta \in [-\pi, \pi],$$

except perhaps for simple eigenvalues

$$(2.11) \quad \lambda = \pm \sqrt{\frac{1}{2}b^2 - a^2},$$

which can only occur if $|a^2| > |\frac{1}{2}b^2 - a^2|$.

Proof. Suppose that z_m is a root of the characteristic polynomial $p_m(z)$ for $m \geq 2$. If $z_m = 0$ then we must have that $a^2 = b^2$. To see this, assume for a contradiction that $a^2 \neq b^2$, then $B(0) \neq 0$ while $A(0) = 0$ and $p_m(0) = 0$ and thus the recurrence relation (2.2) gives that $p_{m-1}(0) = 0$. Following this recursion down to $m = 2$ gives that $p_1(0) = 0$, which is false as $b \neq 0$. Further, if $p_m(0) = 0$ then also $p_{m+1}(0) = 0$ by (2.2) since $A(0) = 0$ and so a sequence of zero roots occurs as m increases giving 0 in the limiting spectrum. This case is covered by choosing $\theta = \frac{\pi}{2}$ in (2.10) and noting that $a^2 = b^2$ must hold. As such, for the remainder of the proof we assume that $z_m \neq 0$.

Now consider the denominator $D(t, z_m)$. Since $A(z_m) \neq 0$ by the assumption that $z_m \neq 0$, the denominator as a quadratic in t has two roots t_1 and t_2 . Note that neither of these two roots can be zero since $t_1 t_2 A(z_m) = 1$, by the definition of t_1 and t_2 as roots of $D(t, z_m)$. If $t_1 = t_2$ then the (regular) discriminant of $D(t, z_m)$ is zero, giving $B(z_m)^2 - 4A(z_m) = 0$. Solving for z_m given our expressions for $A(z)$ and $B(z)$ yields solutions $z_m = \pm(a \pm b)$ for all choices of signs. These cases are also covered by (2.10) when $\theta = 0$ or $\theta = \pi$.

As such, we now assume that $t_1 \neq t_2$ and so $D(t, z_m) = A(z_m)(t - t_1)(t - t_2)$. Considering the generating function (2.3) we observe that

$$(2.12) \quad \begin{aligned} \frac{N(t, z_m)}{D(t, z_m)} &= \frac{1 - a^2 t}{A(z_m)(t - t_1)(t - t_2)} = \frac{1 - a^2 t}{A(z_m)(t_1 - t_2)} \left(\frac{1}{t - t_1} - \frac{1}{t - t_2} \right) \\ &= \frac{1 - a^2 t}{A(z_m)(t_1 - t_2)} \sum_{m=0}^{\infty} \frac{t_1^{m+1} - t_2^{m+1}}{t_1^{m+1} t_2^{m+1}} t^m \\ &= \frac{1}{A(z_m)(t_1 - t_2)} \sum_{m=1}^{\infty} \left[\frac{t_1^{m+1} - t_2^{m+1}}{t_1^{m+1} t_2^{m+1}} - a^2 \frac{t_1^m - t_2^m}{t_1^m t_2^m} \right] t^m + 1. \end{aligned}$$

Thus, if z_m is a root of $p_m(z)$ then the coefficient of t^m in (2.12) must be zero. Now suppose $t_1 = q t_2$ for some $q \neq 0$ (as neither t_1 nor t_2 is zero), then this condition on the coefficient of t^m translates into

$$\frac{q^{m+1} - 1}{q^{m+1} t_2^{m+1}} - a^2 \frac{q^m - 1}{q^m t_2^m} = 0 \implies q^{m+1} - 1 = a^2 t_2 q (q^m - 1).$$

We will later use the q -discriminant condition (2.9) for $D(t, z_m)$ to characterise the root z_m as $m \rightarrow \infty$, noting that (2.9) holds precisely when q is as defined above. For now, since $t_1 t_2 A(z_m) = 1$, we deduce that $t_2 = \pm(A(z_m) q)^{-1/2}$ and thus q must solve

$$(q^{m+1} - 1)^2 = \frac{a^4}{A(z_m)} (q^m - 1)^2 q.$$

Let us define the coefficient, depending on z_m ,

$$(2.13) \quad c_m = \frac{a^4}{A(z_m)} = \frac{a^2}{z_m^2}.$$

Then q must be a root of the $2m + 2$ degree polynomial

$$(2.14) \quad f_m(q) = q^{2m+2} - c_m q^{2m+1} + 2(c_m - 1)q^{m+1} - c_m q + 1.$$

In order to characterise the roots of (2.14) we will make use of the following corollary of Rouché's theorem: for a polynomial f of degree d with coefficients $\{\alpha_j\}_{j=0}^d$, if $R > 0$ is such that for an integer $0 \leq k \leq d$ we have

$$(2.15) \quad |\alpha_k|R^k > |\alpha_0| + \dots + |\alpha_{k-1}|R^{k-1} + |\alpha_{k+1}|R^{k+1} + \dots + |\alpha_d|R^d,$$

then there are exactly k roots of f , counted with multiplicity, having absolute value less than R . In particular, we will use this result for the polynomial $f_m(q)$ with $k = 0$ or $k = 1$.

We first point out some facts about (2.14). Note that $q = 0$ is not a root of f_m and, moreover, by symmetry of the coefficients, if q_m is a root of f_m then

$$f_m(q_m^{-1}) = q_m^{-(2m+2)} f_m(q_m) = 0$$

and so q_m^{-1} is also a root. In particular, note that all such q_m^{-1} satisfy the same polynomial (2.14) and thus the multiplicities of the roots q_m and q_m^{-1} are identical. This means that we only need to study roots with $|q_m| \leq 1$, with roots outside the unit disc being precisely the reciprocal values of those inside the unit disc.

We will use (2.15) to determine how many roots of $f_m(q)$ in (2.14) do not approach the unit circle as $m \rightarrow \infty$. This information, along with (2.9), will allow us to determine conditions for z_m . A significant challenge is that the coefficient c_m depends on m , and so we must consider the behaviour of the sequence (c_m) . Specifically, let (\hat{c}_m) be a subsequence of c_m values and suppose it falls into one of the four cases:

1. (\hat{c}_m) is such that $|\hat{c}_m| \rightarrow \infty$,
2. (\hat{c}_m) is such that there exists c and C fixed with $1 < c \leq |\hat{c}_m| \leq C$,
3. (\hat{c}_m) is such that $|\hat{c}_m| \rightarrow 1$ from above,
4. (\hat{c}_m) is such that $|\hat{c}_m| \leq 1$.

Note that any sequence (c_m) may feature a combination of different subsequence cases but must contain a subsequence of at least one type. Further, all other subsequences must be a combination of the four cases above. We will show that all cases lead to the conclusion that all but possibly two roots of $f_m(q)$ tend to the unit circle. The two separate roots only persist in cases 1 and 2 and, moreover, case 1 only occurs in a very specific situation which results in zero being in the limiting spectrum of \mathcal{T} .

Case 1. To start the analysis we suppose we are in case 1 where $|\hat{c}_m| \rightarrow \infty$ and consider the required inequality (2.15) to apply the corollary of Rouché's theorem. Let $R = 2^{-2/m}$ then we have that

$$\begin{aligned} & 1 + 2|c_m - 1|R^{m+1} + |c_m|R^{2m+1} + R^{2m+2} \\ & \leq 1 + 2(|c_m| + 1)2^{-2-2/m} + |c_m|2^{-4-2/m} + 2^{-4-4/m} \\ & = |c_m|2^{-2/m} \left(2^{-1} + 2^{-4} + |c_m|^{-1}(2^{2/m} + 2^{-1} + 2^{-4-2/m}) \right) \\ & < |c_m|R, \end{aligned}$$

where the final inequality is true for all $m \geq 2$ when $|c_m| > \frac{81}{14}$. Thus, for large enough m , there is only a single root s_m such that $|s_m| < 2^{-2/m}$ and it is simple. As $m \rightarrow \infty$ this shows that all but two roots, s_m and s_m^{-1} , tend to one in modulus.

We now investigate the behaviour of s_m and s_m^{-1} . Let $R = 2|c_m|^{-1}$ and suppose, w.l.o.g., that $|c_m| \geq 4$ and $m \geq 4$. Then we have that

$$\begin{aligned} & 1 + 2|c_m - 1|R^{m+1} + |c_m|R^{2m+1} + R^{2m+2} \\ & \leq 1 + 2(|c_m| + 1)\frac{2^{m+1}}{|c_m|^{m+1}} + \frac{2^{2m+1}}{|c_m|^{2m}} + \frac{2^{2m+2}}{|c_m|^{2m+2}} \\ & \leq 1 + 2\left(2^{-(m-1)} + 2^{-(m+1)}\right) + 2^{-(2m-1)} + 2^{-(2m+2)} \\ & < 1 + 2^{3-m} \\ & < |c_m|R, \end{aligned}$$

and so we deduce that s_m is such that $|s_m| < 2|c_m|^{-1}$ for large enough m , showing that $s_m \rightarrow 0$ as $m \rightarrow \infty$. This bound on $|s_m|$ gives that

$$s_m^{2m+2} - c_m s_m^{2m+1} + 2(c_m - 1)s_m^{m+1} \rightarrow 0.$$

Hence, since $f_m(s_m) = 0$ for all m , we must have that $1 - c_m s_m \rightarrow 0$ and thus $s_m - c_m^{-1} \rightarrow 0$ as $m \rightarrow \infty$. We would now like to interpret what this shows for the corresponding root z_m using the q -discriminant condition (2.9) but we cannot simply insert $q = 0$ and taking the limit $q = s_m \rightarrow 0$ shows that $z_m \rightarrow 0$ which can already be deduced from the fact that $|c_m| \rightarrow \infty$. Instead, we use the definition (2.13) of $c_m = a^2/z_m^2$ and denote $\delta_m = c_m s_m - 1$ where $\delta_m \rightarrow 0$ as $m \rightarrow \infty$. Then, with $q = s_m = c_m^{-1}(1 + \delta_m)$, (2.9) becomes

$$\begin{aligned} & \frac{B(z_m)^2}{A(z_m)} = c_m^{-1}(1 + \delta_m) + c_m(1 + \delta_m)^{-1} + 2 \\ \iff & \frac{(-z_m^2 + b^2 - a^2)^2}{a^2 z_m^2} = \frac{z_m^2}{a^2}(1 + \delta_m) + \frac{a^2}{z_m^2}(1 + \delta_m)^{-1} + 2 \\ (2.16) \iff & b^4 - 2a^2 b^2 - 2b^2 z_m^2 = \delta_m(z_m^4 - a^4) + \mathcal{O}(\delta_m^2), \end{aligned}$$

where we have used the binomial expansion $(1 + \delta_m)^{-1} = 1 - \delta_m + \mathcal{O}(\delta_m^2)$, which is valid for large m since $\delta_m \rightarrow 0$. Now note that (2.16) is a singular perturbation and as $\delta_m \rightarrow 0$ all roots z_m go to infinity except for those which satisfy the left-hand side being zero, namely we have the limiting roots

$$(2.17) \quad z = \pm \sqrt{\frac{1}{2}b^2 - a^2}.$$

Now since $z_m \rightarrow 0$ by the assumption that $|c_m| \rightarrow \infty$, this case of unbounded c_m can only occur when the limiting roots defined in (2.17) are zero, that is when $a^2 = \frac{1}{2}b^2$.

Case 2. We now turn to the analysis of case 2 where $1 < c \leq |\hat{c}_m| \leq C$ and let $\varepsilon > 0$ be small. Suppose, w.l.o.g., that $c \geq \frac{1+\varepsilon}{1-\varepsilon}$, or else take a smaller ε . Now consider $R = 1 - \varepsilon$ and let M_C be such that

$$2(C + 1)R^{m+1} + CR^{2m+1} + R^{2m+2} < \varepsilon$$

for all $m \geq M_C$. Then

$$\begin{aligned} 1 + 2|c_m - 1|R^{m+1} + |c_m|R^{2m+1} + R^{2m+2} & \leq 1 + 2(C + 1)R^{m+1} + CR^{2m+1} + R^{2m+2} \\ & < 1 + \varepsilon \\ & \leq |c_m|R \end{aligned}$$

for $m \geq M_C$. Thus there is only a single root s_m with modulus less than R and it is simple. Since $\varepsilon > 0$ was arbitrary, taking the limit $\varepsilon \rightarrow 0$ so that $R \rightarrow 1$ shows that all remaining roots of f_m tend to one in modulus. Now let $R = (1 + \varepsilon)c^{-1}$ with ε small enough so that $R < 1$, then the same argument above applies similarly. As such, for large enough m , taking $\varepsilon = \frac{c-1}{c+1}$ shows that $|s_m| < \frac{2}{c+1} < 1$. Since $|s_m|$ is bounded away from one, an identical argument to that made in case 1 shows that $s_m - c_m^{-1} \rightarrow 0$ as $m \rightarrow \infty$ and so the corresponding $z_m = \sqrt{a^2/c_m}$ must tend to the limiting roots in (2.17), but now these roots cannot be zero as $|c_m|$ is bounded. Furthermore, since we are considering case 2 we require $|c_m| > 1$, and so $|a^2| > |z_m^2|$, to hold for arbitrarily large m . For this to hold in the limit we require $|a^2| > |\frac{1}{2}b^2 - a^2|$.

Case 3. Consider now case 3, where $|\hat{c}_m| \rightarrow 1$ from above, and let $\varepsilon > 0$ be small. Let $R = 1 - \varepsilon$, and define $\bar{C} = \max_m |c_m|$, \bar{M} such that

$$2(\bar{C} + 1)R^{m+1} + \bar{C}R^{2m+1} + R^{2m+2} < \frac{\varepsilon}{2}$$

for all $m \geq \bar{M}$, and \hat{M} such that

$$|c_m| \leq \frac{1 - \frac{\varepsilon}{2}}{1 - \varepsilon}$$

for all $m \geq \hat{M}$. Then,

$$\begin{aligned} & |c_m|R + 2|c_m - 1|R^{m+1} + |c_m|R^{2m+1} + R^{2m+2} \\ & \leq \frac{1 - \frac{\varepsilon}{2}}{1 - \varepsilon}R + 2(\bar{C} + 1)R^{m+1} + \bar{C}R^{2m+1} + R^{2m+2} \\ & < 1, \end{aligned}$$

for all $m \geq \max\{\bar{M}, \hat{M}\}$. Thus, for large enough m , there are no roots of f_m with modulus less than $R = 1 - \varepsilon$. Since $\varepsilon > 0$ was arbitrary, taking the limit $\varepsilon \rightarrow 0$ so that $R \rightarrow 1$ shows that all roots of f_m tend to one in modulus.

Case 4. Finally, consider case 4 where $|\hat{c}_m| \leq 1$. Let $\varepsilon > 0$ be small, and define $R = 1 - \varepsilon$. Let M_1 be such that

$$4R^{m+1} + R^{2m+1} + R^{2m+2} < \varepsilon$$

for all $m \geq M_1$. Then we have that

$$\begin{aligned} |c_m|R + 2|c_m - 1|R^{m+1} + |c_m|R^{2m+1} + R^{2m+2} & \leq R + 4R^{m+1} + R^{2m+1} + R^{2m+2} \\ & < 1, \end{aligned}$$

for $m \geq M_1$. Thus, as in case 3, we deduce that all roots of f_m tend to one in modulus as $m \rightarrow \infty$.

We have already seen that in cases 1 and 2 we have simple roots z_m which tend to the limiting values in (2.17) when $|a^2| > |\frac{1}{2}b^2 - a^2|$. In all cases, and thus all sequences of possible c_m values, all remaining roots z_m correspond to q values which tend to the unit circle. Thus z_m must tend to the limiting curve defined by (2.9) where $q = e^{i\phi}$ for some $\phi \in [-\pi, \pi]$. This limiting curve in the complex plane is given parametrically

as

$$\begin{aligned}
\frac{B(z)^2}{A(z)} &= e^{i\phi} + e^{-i\phi} + 2, & \phi &\in [-\pi, \pi] \\
\iff \frac{(-z^2 + b^2 - a^2)^2}{a^2 z^2} &= 4 \cos^2\left(\frac{\phi}{2}\right), & \phi &\in [-\pi, \pi] \\
\iff z^2 - b^2 + a^2 &= \pm 2az \cos\left(\frac{\phi}{2}\right), & \phi &\in [-\pi, \pi] \\
\iff z^2 - 2a \cos(\theta)z - b^2 + a^2 &= 0, & \theta &\in [-\pi, \pi] \\
\iff z = a \cos(\theta) \pm \sqrt{b^2 - a^2 \sin^2(\theta)}, & & \theta &\in [-\pi, \pi].
\end{aligned}$$

Thus, as roots z_m of $p_m(z)$ are eigenvalues λ of $\mathcal{T} \in \mathbb{C}^{2m \times 2m}$, we deduce that the limiting spectra of \mathcal{T} lies on the curve defined by (2.10) as $m \rightarrow \infty$, except perhaps for simple eigenvalues (2.11) which can only occur if $|a^2| > |\frac{1}{2}b^2 - a^2|$. \square

We note that, while the so-called Szegő formula does not apply in our non-Hermitian case, we have just proven that all eigenvalues of \mathcal{T} , except perhaps two, lie on the equivalent curve defined by eigenvalues of the (block) symbol of \mathcal{T} , which is precisely that defined in (2.10).

3. The one-dimensional problem. We now turn our attention to analysing the one-level method. In this section we study the parallel Schwarz iterative method for the one-dimensional Maxwell's equations with Robin boundary conditions defined on the domain $\Omega = (a_1, b_N)$:

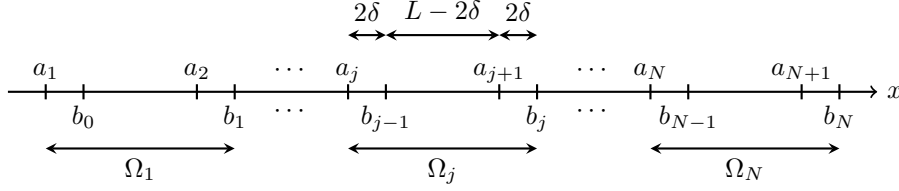
$$(3.1) \quad \begin{cases} \mathcal{L}u := -\partial_{xx}u + (ik\tilde{\sigma} - k^2)u = 0, & x \in (a_1, b_N), \\ \mathcal{B}_l u := -\partial_x u + \alpha u = g_1, & x = a_1, \\ \mathcal{B}_r u := \partial_x u + \alpha u = g_2, & x = b_N, \end{cases}$$

where u represents the complex amplitude of the electric field, k is the wave number, and $\tilde{\sigma} = \sigma Z$ with σ being the conductivity of the medium and Z its impedance. Here α is the impedance parameter which is chosen such that the local problems are well-posed and is classically set to ik , in which case the problem corresponds to a “one-dimensional wave-guide” and the incoming wave or excitation can be represented by g_1 , for example, with g_2 being set to 0. Note that, when $\alpha = ik$, the problem is well-posed even if $\tilde{\sigma} = 0$ but in the following we will assume that $\tilde{\sigma} > 0$. In order to simplify notation we will omit the tilde symbol for σ . We remark that (3.1) can also be seen as an absorptive Helmholtz equation where the absorption term $ik\sigma$ comes from the physics of the problem.

Let us also consider two sets of points $\{a_j\}_{j=1, \dots, N+1}$ and $\{b_j\}_{j=0, \dots, N}$ defining the overlapping decomposition $\Omega = \cup_{j=1}^N \Omega_j$ such that $\Omega_j = (a_j, b_j)$, as illustrated in Figure 3.1 (and considered in [4]), where

$$(3.2) \quad b_j - a_j = L + 2\delta, \quad b_{j-1} - a_j = 2\delta, \quad a_{j+1} - a_j = b_{j+1} - b_j = L, \quad \delta > 0.$$

Note that the length of each subdomain is fixed and equal to $L + 2\delta$ while the overlap is always 2δ . We consider solving (3.1) by a Schwarz iterative algorithm and denote by u_j^n the approximation to the solution in subdomain j at iteration n , starting from an initial guess u_j^0 . We compute u_j^n from the previous values u_j^{n-1} by solving the

FIG. 3.1. Overlapping decomposition of the one-dimensional domain into N subdomains.

following local boundary value problem

$$(3.3a) \quad \begin{cases} \mathcal{L}u_j^n = 0, & x \in \Omega_j, \\ \mathcal{B}_l u_j^n = \mathcal{B}_l u_{j-1}^{n-1}, & x = a_j, \\ \mathcal{B}_r u_j^n = \mathcal{B}_r u_{j+1}^{n-1}, & x = b_j, \end{cases}$$

in the case $2 \leq j \leq N$ while for the first ($j = 1$) and last ($j = N$) subdomain we have

$$(3.3b) \quad \begin{cases} \mathcal{L}u_1^n = 0, & x \in \Omega_1, \\ \mathcal{B}_l u_1^n = g_1, & x = a_1, \\ \mathcal{B}_r u_1^n = \mathcal{B}_r u_2^{n-1}, & x = b_1, \end{cases} \quad \begin{cases} \mathcal{L}u_N^n = 0, & x \in \Omega_N, \\ \mathcal{B}_l u_N^n = \mathcal{B}_l u_{N-1}^{n-1}, & x = a_N, \\ \mathcal{B}_r u_N^n = g_2, & x = b_N. \end{cases}$$

In the following we wish to analyse the convergence of the iterative method defined in (3.3), which is also called the *parallel Schwarz method*, for a growing number of subdomains N and for the absorptive problem, i.e. $\sigma > 0$.¹

In order to do this we define the local errors in each subdomain j at iteration n as $e_j^n = u|_{\Omega_j} - u_j^n$. They verify the boundary value problems (3.3a) for the interior subdomains and the homogeneous analogues of (3.3b) for the first and last subdomains (i.e. (3.3b) but with boundary conditions $g_1 = 0$ and $g_2 = 0$). The convergence study will be done in two steps: first we prove that the Schwarz iteration matrix is a block Toeplitz matrix and then that its spectral radius is less than one.

LEMMA 3.1 (Block Toeplitz iteration matrix). *If $e_j^n = u|_{\Omega_j} - u_j^n$ is the local error in each subdomain j at iteration n and*

$$\mathcal{R}^n := [\mathcal{R}_+^n(b_1), \mathcal{R}_-^n(a_2), \mathcal{R}_+^n(b_2), \dots, \mathcal{R}_-^n(a_{N-1}), \mathcal{R}_+^n(b_{N-1}), \mathcal{R}_-^n(a_N)]^T,$$

where

$$(3.4) \quad \mathcal{R}_-^n(a_j) := \mathcal{B}_l e_{j-1}^n(a_j), \quad \mathcal{R}_+^n(b_j) := \mathcal{B}_r e_{j+1}^n(b_j),$$

is the Robin interface data, then

$$\mathcal{R}^n = \mathcal{T}_{1d} \mathcal{R}^{n-1},$$

where \mathcal{T}_{1d} is a block Toeplitz matrix of the form (2.1) with a and b given by

$$(3.5a) \quad a = \frac{(\zeta + \alpha)^2 e^{2\zeta\delta} - (\zeta - \alpha)^2 e^{-2\zeta\delta}}{(\zeta + \alpha)^2 e^{\zeta(2\delta+L)} - (\zeta - \alpha)^2 e^{-\zeta(2\delta+L)}},$$

$$(3.5b) \quad b = -\frac{(\zeta^2 - \alpha^2)(e^{\zeta L} - e^{-\zeta L})}{(\zeta + \alpha)^2 e^{\zeta(2\delta+L)} - (\zeta - \alpha)^2 e^{-\zeta(2\delta+L)}},$$

where $\zeta = \sqrt{ik\sigma - k^2}$.

¹When $\sigma = 0$, impedance transmission conditions are also transparent conditions, with the resulting iteration matrix being nilpotent. Therefore, the algorithm will converge in a number of iterations equal to the number of subdomains in this case.

Proof. We first see that the solution to $\mathcal{L}e_j^n = 0$ is given by

$$(3.6) \quad e_j^n(x) = \alpha_j^n e^{-\zeta x} + \beta_j^n e^{\zeta x}, \quad \zeta = \sqrt{ik\sigma - k^2}.$$

Note that we choose the principle branch of the square root here so that ζ always has positive real and imaginary parts. Now the interface iterations at $x = a_j$ and $x = b_j$ from (3.3) can be written in terms of the error as

$$(3.7) \quad \begin{bmatrix} \mathcal{B}_l e_j^n(a_j) \\ \mathcal{B}_r e_j^n(b_j) \end{bmatrix} = \begin{bmatrix} \mathcal{B}_l e_{j-1}^{n-1}(a_j) \\ \mathcal{B}_r e_{j+1}^{n-1}(b_j) \end{bmatrix}.$$

By introducing (3.6) into the left-hand side of (3.7) and by using the notation from (3.4) we obtain

$$\begin{bmatrix} (\zeta + \alpha)e^{-\zeta a_j} & -(\zeta - \alpha)e^{\zeta a_j} \\ -(\zeta - \alpha)e^{-\zeta b_j} & (\zeta + \alpha)e^{\zeta b_j} \end{bmatrix} \begin{bmatrix} \alpha_j^n \\ \beta_j^n \end{bmatrix} = \begin{bmatrix} \mathcal{R}_-^{n-1}(a_j) \\ \mathcal{R}_+^{n-1}(b_j) \end{bmatrix},$$

which we can solve for the unknowns α_j^n and β_j^n to give

$$(3.8) \quad \begin{bmatrix} \alpha_j^n \\ \beta_j^n \end{bmatrix} = \frac{1}{D_j} \begin{bmatrix} (\zeta + \alpha)e^{\zeta b_j} & (\zeta - \alpha)e^{\zeta a_j} \\ (\zeta - \alpha)e^{-\zeta b_j} & (\zeta + \alpha)e^{-\zeta a_j} \end{bmatrix} \begin{bmatrix} \mathcal{R}_-^{n-1}(a_j) \\ \mathcal{R}_+^{n-1}(b_j) \end{bmatrix},$$

where $D_j = (\zeta + \alpha)^2 e^{\zeta(b_j - a_j)} - (\zeta - \alpha)^2 e^{\zeta(a_j - b_j)}$. Note that, since $b_j - a_j = L + 2\delta$, then D_j is actually independent of j and thus we simply denote it by D . The algorithm is based on Robin transmission conditions, hence the quantities of interest which are transmitted at the interfaces between subdomains are the Robin data (3.4). Therefore, we need to compute the current interface values $\mathcal{R}_-^n(a_j)$ and $\mathcal{R}_+^n(b_j)$ by replacing the coefficients from (3.8) into (3.6) and then applying the formulae in (3.4), giving

$$(3.9a) \quad \begin{aligned} \mathcal{R}_-^n(a_j) &= \mathcal{B}_l e_{j-1}^n(a_j) = (\zeta + \alpha)\alpha_{j-1}^n e^{-\zeta a_j} - (\zeta - \alpha)\beta_{j-1}^n e^{\zeta a_j} \\ &= \frac{1}{D} \left[((\zeta + \alpha)^2 e^{\zeta(b_{j-1} - a_j)} - (\zeta - \alpha)^2 e^{\zeta(a_j - b_{j-1})}) \mathcal{R}_-^{n-1}(a_{j-1}) \right. \\ &\quad \left. + (\zeta^2 - \alpha^2)(e^{\zeta(a_{j-1} - a_j)} - e^{\zeta(a_j - a_{j-1})}) \mathcal{R}_+^{n-1}(b_{j-1}) \right], \end{aligned}$$

$$(3.9b) \quad \begin{aligned} \mathcal{R}_+^n(b_j) &= \mathcal{B}_r e_{j+1}^n(b_j) = -(\zeta - \alpha)\alpha_{j+1}^n e^{-\zeta b_j} + (\zeta + \alpha)\beta_{j+1}^n e^{\zeta b_j} \\ &= \frac{1}{D} \left[(\zeta^2 - \alpha^2)(e^{\zeta(b_j - b_{j+1})} - e^{\zeta(b_{j+1} - b_j)}) \mathcal{R}_-^{n-1}(a_{j+1}) \right. \\ &\quad \left. + ((\zeta + \alpha)^2 e^{\zeta(b_j - a_{j+1})} - (\zeta - \alpha)^2 e^{\zeta(a_{j+1} - b_j)}) \mathcal{R}_+^{n-1}(b_{j+1}) \right]. \end{aligned}$$

The iteration of interface values (3.9) can be summarised as follows:

$$(3.10a) \quad \begin{bmatrix} \mathcal{R}_-^n(a_j) \\ \mathcal{R}_+^n(b_j) \end{bmatrix} = T_1 \begin{bmatrix} \mathcal{R}_-^{n-1}(a_{j-1}) \\ \mathcal{R}_+^{n-1}(b_{j-1}) \end{bmatrix} + T_2 \begin{bmatrix} \mathcal{R}_-^{n-1}(a_{j+1}) \\ \mathcal{R}_+^{n-1}(b_{j+1}) \end{bmatrix},$$

$$T_1 = \begin{bmatrix} a & b \\ 0 & 0 \end{bmatrix}, \quad T_2 = \begin{bmatrix} 0 & 0 \\ b & a \end{bmatrix},$$

where a and b are given by (3.5). Note that since the homogeneous counterparts of the boundary conditions from (3.3b) translate into $\mathcal{R}_-^n(a_1) = 0$ and $\mathcal{R}_+^n(b_N) = 0$ for all n , we can remove these terms. As such, the iterates for $j \in \{1, 2, N-1, N\}$ are

prescribed slightly differently as

$$(3.10b) \quad \begin{aligned} \begin{bmatrix} 0 \\ \mathcal{R}_+^n(b_1) \end{bmatrix} &= T_2 \begin{bmatrix} \mathcal{R}_+^{n-1}(a_2) \\ \mathcal{R}_+^{n-1}(b_2) \end{bmatrix}, \\ \begin{bmatrix} \mathcal{R}_-^n(a_2) \\ \mathcal{R}_+^n(b_2) \end{bmatrix} &= T_1 \begin{bmatrix} 0 \\ \mathcal{R}_+^{n-1}(b_1) \end{bmatrix} + T_2 \begin{bmatrix} \mathcal{R}_+^{n-1}(a_3) \\ \mathcal{R}_+^{n-1}(b_3) \end{bmatrix}, \\ \begin{bmatrix} \mathcal{R}_-^n(a_{N-1}) \\ \mathcal{R}_+^n(b_{N-1}) \end{bmatrix} &= T_1 \begin{bmatrix} \mathcal{R}_+^{n-1}(a_{N-2}) \\ \mathcal{R}_+^{n-1}(b_{N-2}) \end{bmatrix} + T_2 \begin{bmatrix} \mathcal{R}_+^{n-1}(a_N) \\ 0 \end{bmatrix}, \\ \begin{bmatrix} \mathcal{R}_-^n(a_N) \\ 0 \end{bmatrix} &= T_1 \begin{bmatrix} \mathcal{R}_+^{n-1}(a_{N-1}) \\ \mathcal{R}_+^{n-1}(b_{N-1}) \end{bmatrix}. \end{aligned}$$

With the notation from (3.4), global iteration over interface data belonging to all subdomains becomes $\mathcal{R}^n = \mathcal{T}_{1d}\mathcal{R}^{n-1}$ where

$$(3.11) \quad \mathcal{T}_{1d} = \begin{bmatrix} 0 & \hat{T}_2 & & & & & & & \\ \tilde{T}_1 & 0_{2 \times 2} & T_2 & & & & & & \\ & \ddots & \ddots & \ddots & & & & & \\ & & T_1 & 0_{2 \times 2} & T_2 & & & & \\ & & & \ddots & \ddots & \ddots & & & \\ & & & & T_1 & 0_{2 \times 2} & \tilde{T}_2 & & \\ & & & & & \hat{T}_1 & 0 & & \end{bmatrix}$$

with $\tilde{T}_1 = [b \ 0]^T$, $\tilde{T}_2 = [0 \ b]^T$, $\hat{T}_1 = [a \ b]$, $\hat{T}_2 = [b \ a]$. We conclude from this that the Schwarz algorithm is given by a stationary iteration with iteration matrix \mathcal{T}_{1d} given by (3.11) and, therefore, convergence is determined by the spectral radius $\rho(\mathcal{T}_{1d})$. We also notice that \mathcal{T}_{1d} is a block Toeplitz matrix of the form (2.1) where a and b are given by (3.5). \square

Before proving convergence of the Schwarz algorithm, we first utilise [Theorem 2.2](#) to provide a useful intermediary result, which will also aid our analysis in the two-dimensional case.

LEMMA 3.2 (Limiting spectral radius and sufficient conditions for convergence).

The following relation holds:

$$\max_{\theta \in [-\pi, \pi]} \left| a \cos(\theta) \pm \sqrt{b^2 - a^2 \sin^2(\theta)} \right| = \max\{|a + b|, |a - b|\},$$

and thus the convergence factor $R_{1d} := \lim_{N \rightarrow \infty} \rho(\mathcal{T}_{1d})$ of the Schwarz algorithm as the number of subdomains tends to infinity verifies

$$(3.12) \quad R_{1d} \leq \begin{cases} \max\{|a + b|, |a - b|\} & \text{if } |a^2 - \frac{1}{2}b^2|^{1/2} \geq |a|, \\ \max\{|a + b|, |a - b|, |a|\} & \text{if } |a^2 - \frac{1}{2}b^2|^{1/2} < |a|. \end{cases}$$

Further, consider the change of variables

$$(3.13) \quad z = 2\delta\zeta, \quad l = \frac{L}{2\delta}, \quad \gamma = 2\delta\alpha, \quad v = \frac{z - \gamma}{z + \gamma},$$

and let $z := x + iy$. Then the condition $g_{\pm}(z; \delta, l) > 0$, where

$$(3.14) \quad g_{\pm}(z; \delta, l) = (e^{2lx} - 1)(e^{2x} - |v|^2) \pm 4 \sin(ly)(\Im v \cos y - \Re v \sin y)e^{x(l+1)},$$

will ensure that $\max\{|a+b|, |a-b|\} < 1$. Similarly, the condition $g(z; \delta, l) > 0$, where

$$(3.15) \quad g(z; \delta, l) = (e^{2lx} - 1)(e^{2x(l+2)} - |v|^4) + 4 \sin(ly) \cdot [((\Re v)^2 - (\Im v)^2) \sin(y(l+2)) - 2\Re v \Im v \cos(y(l+2))] e^{2x(l+1)},$$

will ensure that $|a| < 1$.

Proof. Since \mathcal{T}_{1d} is of the form \mathcal{T} in (2.1), Theorem 2.2 provides its limiting spectrum and thus allows us to bound R_{1d} by the largest eigenvalue in magnitude. We first bound $\lambda_{\pm}(\theta) = a \cos(\theta) \pm \sqrt{b^2 - a^2 \sin^2(\theta)}$. It is straightforward to see that these values are the eigenvalues of the matrix

$$T = \begin{pmatrix} a \cos(\theta) & b - a \sin(\theta) \\ b + a \sin(\theta) & a \cos(\theta) \end{pmatrix}.$$

A simple computation shows that the matrix

$$T^*T = \begin{pmatrix} |a|^2 + |b|^2 + (a\bar{b} + \bar{a}b) \sin(\theta) & (a\bar{b} + \bar{a}b) \cos(\theta) \\ (a\bar{b} + \bar{a}b) \cos(\theta) & |a|^2 + |b|^2 - (a\bar{b} + \bar{a}b) \sin(\theta) \end{pmatrix}$$

has the eigenvalues $\mu_{\pm} = |a \pm b|^2$. We can now conclude that

$$|\lambda_{\pm}(\theta)| \leq \|T\| = \sqrt{\|T^*T\|} = \sqrt{\max\{\mu_+, \mu_-\}} = \max\{|a+b|, |a-b|\}.$$

Additionally, Theorem 2.2 states that eigenvalues $\lambda = \pm(\frac{1}{2}b^2 - a^2)^{1/2}$ may belong to the limiting spectrum but only if they have magnitude strictly less than $|a|$. Together, these two cases yield (3.12).

Let us consider now the complex valued functions $F_{\pm}: \mathbb{C} \rightarrow \mathbb{C}$

$$F_{\pm}(z) = \frac{(z+\gamma)^2 e^z - (z-\gamma)^2 e^{-z}}{(z+\gamma)^2 e^{(l+1)z} - (z-\gamma)^2 e^{-(l+1)z}} \pm \frac{(z^2 - \gamma^2)(e^{lz} - e^{-lz})}{(z+\gamma)^2 e^{(l+1)z} - (z-\gamma)^2 e^{-(l+1)z}}.$$

It is easy to see that $a \mp b = F_{\pm}(z)$ when z, l and γ are as defined in (3.13). Similarly, we define the function $G: \mathbb{C} \rightarrow \mathbb{C}$ to be the first term in $F_{\pm}(z)$ so that $a = G(z)$. Let us simplify in the first instance the expression of $|F_{\pm}(z)|$ without using any assumption on $z := x + iy$. For this we consider the transformation v along with its polar form

$$(3.16) \quad v := \frac{z - \gamma}{z + \gamma}, \quad v = w(\cos(\varphi) + i \sin(\varphi)), \quad w = |v|.$$

After some lengthy but elementary calculations we find that

$$(3.17a) \quad |F_{\pm}(z)|^2 = 1 - \frac{(e^{x(l+1)} - w)^2 + 2w(1 \mp \cos((l+1)y - \varphi))e^{x(l+1)}}{(e^{2x(l+1)} - w^2)^2 + 4w^2 \sin^2((l+1)y - \varphi)e^{2x(l+1)}} g_{\pm}(z; \delta, l)$$

$$(3.17b) \quad g_{\pm}(z; \delta, l) = (e^{2lx} - 1)(e^{2x} - w^2) \pm 4w \sin(ly) \sin(\varphi - y) e^{x(l+1)}.$$

We observe that the fraction in (3.17a) is positive, since the individual terms involved are, and thus $\max\{|a-b|, |a+b|\} < 1 \Leftrightarrow |F_{\pm}(z)|^2 < 1 \Leftrightarrow g_{\pm}(z; \delta, l) > 0$. We can now rewrite $g_{\pm}(z; \delta, l)$ in (3.17b) using (3.16) and convert v to Cartesian form to obtain the required expression in (3.14). A near identical argument can be used to derive conditions for $|G(z)|^2 < 1$ and results in the criterion that $g(z; \delta, l) > 0$, where $g(z; \delta, l)$ is defined by (3.15). Thus the required conclusions follow. \square

We are now ready to state our main convergence result for the one-dimensional problem in the case when $\alpha = ik$, namely that of classical impedance conditions.

THEOREM 3.3 (Convergence of the Schwarz algorithm in 1D). *If $\alpha = ik$ (the case of classical impedance conditions), then for all $k > 0$, $\sigma > 0$, $\delta > 0$ and $L > 0$ we have that $R_{1d} < 1$. Therefore the convergence will ultimately be independent of the number of subdomains (we say that the Schwarz method will scale).*

Proof. By **Lemma 3.2** we see that it is enough to study the sign of $g_{\pm}(z; \delta, l)$ and of $g(z; \delta, l)$. We can see that if $\alpha = ik$ and $\kappa = 2\delta k$ then for $z := x + iy$ (3.16) becomes

$$\Re v = \frac{-\kappa^2 + x^2 + y^2}{(\kappa + y)^2 + x^2}, \quad \Im v = \frac{-2\kappa x}{(\kappa + y)^2 + x^2}, \quad |v|^2 = \frac{(\kappa - y)^2 + x^2}{(\kappa + y)^2 + x^2} < 1,$$

the final inequality holding since $\kappa > 0$ and $y > 0$. We emphasise that x and y are the real and imaginary parts of $z = 2\delta\zeta$ and so are positive by the nature of ζ in (3.6). Now we can further simplify (3.14) using these expressions for v to obtain

$$(3.18a) \quad g_{\pm}(z; \delta, l) = \frac{4e^{x(l+1)}}{(\kappa + y)^2 + x^2} \tilde{g}_{\pm}(z; \delta, l)$$

$$(3.18b) \quad \tilde{g}_{\pm}(z; \delta, l) = [(\kappa^2 + x^2 + y^2) \sinh(x) + 2\kappa y \cosh(x)] \sinh(lx) \\ \pm [(\kappa^2 - x^2 - y^2) \sin(y) - 2\kappa x \cos(y)] \sin(ly).$$

Proving positivity of $g_{\pm}(z; \delta, l)$ is then equivalent to positivity of $\tilde{g}_{\pm}(z; \delta, l)$. To proceed we relate x and y by considering the real part of $z^2 = (x + iy)^2 = 2i\kappa\delta\sigma - \kappa^2$ which yields $y^2 = \kappa^2 + x^2$. Let us now eliminate y using this identity to obtain

$$\tilde{g}_{\pm}(z; \delta, l) = 2 \left[(\kappa^2 + x^2) \sinh(x) + \kappa \sqrt{\kappa^2 + x^2} \cosh(x) \right] \sinh(lx) \\ \mp 2 \left[x^2 \sin(\sqrt{\kappa^2 + x^2}) + \kappa x \cos(\sqrt{\kappa^2 + x^2}) \right] \sin(l\sqrt{\kappa^2 + x^2}).$$

To show that this is positive we want to lower bound the hyperbolic term in the first line (which is positive) while making the trigonometric term in the second line as large as possible in magnitude and negative. To do this we make use of some elementary bounds which hold for $t > 0$:

$$(3.19) \quad |\sin(t)| < t < \sinh(t), \quad |\cos(t)| \leq 1 < \cosh(t).$$

We can now derive the positivity bound on $\tilde{g}_{\pm}(z; \delta, l)$, noting that $x > 0$, as follows

$$\tilde{g}_{\pm}(z; \delta, l) > 2 \left[(\kappa^2 + x^2)x + \kappa \sqrt{\kappa^2 + x^2} \right] lx - 2 \left[x^2 \sqrt{\kappa^2 + x^2} + \kappa x \right] l \sqrt{\kappa^2 + x^2} = 0.$$

Turning to $g(z; \delta, l)$, we can follow a similar process, simplifying (3.15) to find that

$$(3.20a) \quad g(z; \delta, l) = \frac{4e^{2x(l+1)}}{((\kappa + y)^2 + x^2)^2} \tilde{g}(z; \delta, l)$$

$$(3.20b) \quad \tilde{g}(z; \delta, l) = [((\kappa^2 + x^2 + y^2)^2 + 4\kappa^2 y^2) \sinh(x(l+2)) \\ + 4\kappa y (\kappa^2 + x^2 + y^2) \cosh(x(l+2))] \sinh(lx) \\ + [(-\kappa^2 + x^2 + y^2)^2 - 4\kappa^2 x^2] \sin(y(l+2)) \\ + 4\kappa x (-\kappa^2 + x^2 + y^2) \cos(y(l+2))] \sin(ly).$$

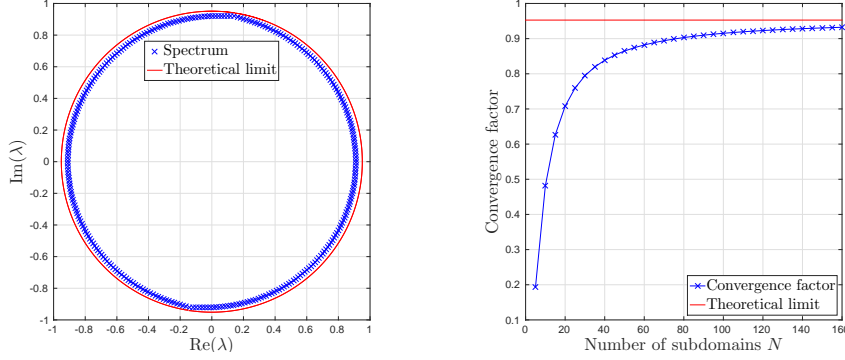


FIG. 3.2. The spectrum of the iteration matrix \mathcal{T}_{1d} for $N = 160$ (left) and the convergence factor of the Schwarz algorithm for varying number of subdomains N (right) when $\sigma = 0.1$.

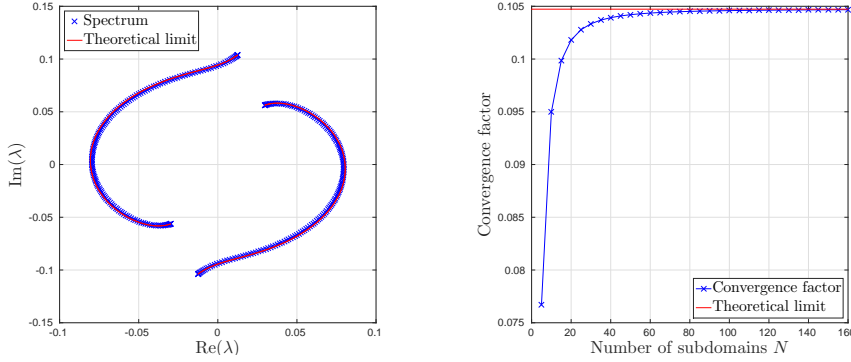


FIG. 3.3. The spectrum of the iteration matrix \mathcal{T}_{1d} for $N = 160$ (left) and the convergence factor of the Schwarz algorithm for varying number of subdomains N (right) when $\sigma = 5$.

Using the identity $y^2 = \kappa^2 + x^2$ along with the elementary bounds (3.19) we obtain

$$\begin{aligned}
 \tilde{g}(z; \delta, l) &= 4 [y^2(y^2 + \kappa^2) \sinh(x(l+2)) + 2\kappa y^3 \cosh(x(l+2))] \sinh(lx) \\
 &\quad + 4 [x^2(x^2 - \kappa^2) \sin(y(l+2)) + 2\kappa x^3 \cos(y(l+2))] \sin(ly) \\
 &> 4 [y^2(y^2 + \kappa^2)x(l+2) + 2\kappa y^3] lx - 4 [x^2(x^2 + \kappa^2)y(l+2) + 2\kappa x^3] ly \\
 &= 4l(l+2)x^2y^2\kappa^2 + 8lxy\kappa^3 \\
 &> 0.
 \end{aligned}$$

Thus, we conclude that for any choice of parameters the required sufficient criteria from Lemma 3.2 on $g_{\pm}(z; \delta, l)$ and $g(z; \delta, l)$ hold and hence $R_{1d} < 1$. Therefore the algorithm will always converge in a number of iterations ultimately independent of the number of subdomains. Nonetheless, note that as any problem parameter shrinks to zero the bounds become tight and so R_{1d} can be made arbitrarily close to one. \square

In order to verify this result, we compute numerically the spectrum of the iteration matrix and compare it with the theoretical limit for different values of σ . We choose here $k = 30$, $L = 1$ and $\delta = L/10$. From Figures 3.2 and 3.3 we notice that the spectrum of the iteration matrix tends to the theoretical limit when the number of subdomains becomes large and the algorithm remains convergent. Additionally, when σ grows the behaviour of the algorithm improves, which is consistent with the fact

that when the absorption in the equations is important (solutions are less oscillatory) or the overlap is large (more information is exchanged) the systems are easier to solve. We also remark an empirical observation that the convergence factor monotonically increases towards the limit given in [Lemma 3.2](#), thus indicating that the algorithm will always converge for any N .

4. The two-dimensional problem. Consider the domain $\Omega = (a_1, b_N) \times (0, \hat{L})$ on which we wish to solve the two-dimensional problem and a decomposition into N overlapping subdomains defined by $\Omega_j = (a_j, b_j) \times (0, \hat{L})$, where a_j and b_j are as given in [\(3.2\)](#). We will analyse the case of the Helmholtz and then Maxwell's equations.

4.1. The Helmholtz equation. The definition of the parallel Schwarz method for the iterates u_j^n in the case of the two-dimensional Helmholtz problem is

$$(4.1) \quad \left\{ \begin{array}{ll} (ik\sigma - k^2)u_j^n - (\partial_{xx} + \partial_{yy})u_j^n = f, & (x, y) \in (a_j, b_j) \times (0, \hat{L}), \\ \mathcal{B}_l u_j^n(a_j, y) = \mathcal{B}_l u_{j-1}^{n-1}(a_j, y), & y \in (0, \hat{L}), \\ \mathcal{B}_r u_j^n(b_j, y) = \mathcal{B}_r u_{j+1}^{n-1}(b_j, y), & y \in (0, \hat{L}), \\ u_j^n(x, y) = 0, & x \in (a_j, b_j), y \in \{0, \hat{L}\}, \end{array} \right.$$

where the boundary operators \mathcal{B}_l and \mathcal{B}_r are as defined in [\(3.1\)](#). We consider here the case of impedance conditions, i.e. $\alpha = ik$. Note that this configuration corresponds to a “two-dimensional wave-guide” problem. By linearity, it follows that the local errors $e_j^n = u|_{\Omega_j} - u_j^n$ satisfy the homogeneous analogue of [\(4.1\)](#). To proceed, we make use of the Fourier sine expansion of e_j^n , as the solution verifies Dirichlet boundary conditions on the top and bottom of each rectangular subdomain:

$$(4.2) \quad e_j^n(x, y) = \sum_{m=1}^{\infty} v_j^n(x, \tilde{k}) \sin(\tilde{k}y), \quad \tilde{k} = \frac{m\pi}{\hat{L}}, \quad m \in \mathbb{N}.$$

Inserting this expression into the homogeneous counterpart of [\(4.1\)](#) we find that, for each Fourier number \tilde{k} , $v_j^n(x, \tilde{k})$ verifies the one-dimensional problem

$$(4.3) \quad \left\{ \begin{array}{ll} (ik\sigma + \tilde{k}^2 - k^2)v_j^n - \partial_{xx}v_j^n = 0, & x \in (a_j, b_j), \\ \mathcal{B}_l v_j^n(x, \tilde{k}) = \mathcal{B}_l v_{j-1}^{n-1}(x, \tilde{k}), & x = a_j, \\ \mathcal{B}_r v_j^n(x, \tilde{k}) = \mathcal{B}_r v_{j+1}^{n-1}(x, \tilde{k}), & x = b_j, \end{array} \right.$$

which is of exactly the same type as [\(3.3\)](#) where $ik\sigma - k^2$ is replaced by $ik\sigma + \tilde{k}^2 - k^2$. Therefore, the result from [Lemma 3.1](#) applies here if we replace α with ik and ζ with

$$(4.4) \quad \zeta(\tilde{k}) = \sqrt{ik\sigma + \tilde{k}^2 - k^2}.$$

Let us denote the resulting iteration matrix, which propagates information for each Fourier number \tilde{k} independently, by $\mathcal{T}_{1d}^H(\tilde{k})$ and let $R_{1d}^H(\tilde{k}) := \lim_{N \rightarrow \infty} \rho(\mathcal{T}_{1d}^H(\tilde{k}))$ with $R_{2d}^H = \sup_{\tilde{k}} R_{1d}^H(\tilde{k})$. We can now state our main convergence result for the two-dimensional Helmholtz problem.

THEOREM 4.1 (Convergence of the Schwarz algorithm for Helmholtz in 2D). *If $\alpha = ik$ (the case of classical impedance conditions), then for all $k > 0$, $\sigma > 0$, $\delta > 0$ and $L > 0$ we have that $R_{1d}^H(\tilde{k}) < 1$ for all evanescent modes $\tilde{k} > k$. Furthermore, under the assumption that between them σ , δ and L are sufficiently large we have that $R_{2d}^H < 1$. In particular, this is true when $\sigma \geq k$ for all $\delta > 0$ and $L > 0$. Therefore the convergence will ultimately be independent of the number of subdomains (we say that the Schwarz method will scale).*

Proof. By Lemma 3.2 we see that it is enough to study the sign of $g_{\pm}(z; \delta, l)$ and $g(z; \delta, l)$. To assist, we use the scaled notation $\kappa = 2\delta k$, $\tilde{\kappa} = 2\delta \tilde{k}$ and $s = 2\delta\sigma$ akin to (3.13). Now $g_{\pm}(z; \delta, l)$ can be formally simplified identically to (3.18), however, in this case with ζ as in (4.4) the real part of z^2 gives the identity $\tilde{\kappa}^2 - \kappa^2 = x^2 - y^2$. Utilising this identity along with the bounds (3.19) yields

$$\begin{aligned} \tilde{g}_{\pm}(z; \delta, l) &> [(\kappa^2 + x^2 + y^2)x + 2\kappa y] lx - |(\kappa^2 - x^2 - y^2)y - 2\kappa x| ly \\ &\geq l(\kappa^2 + x^2 + y^2)(\tilde{\kappa}^2 - \kappa^2). \end{aligned}$$

Hence we always have $\tilde{g}_{\pm}(z; \delta, l) > 0$ for the evanescent modes $\tilde{k} > k$ (equivalent to $\tilde{\kappa} > \kappa$). Similarly, $g(z; \delta, l)$ can be simplified identically to (3.20) and we find that

$$\begin{aligned} \tilde{g}(z; \delta, l) &> l(l+2) (x^2((\kappa^2 + x^2 + y^2)^2 + 4\kappa^2 y^2) - y^2|(-\kappa^2 + x^2 + y^2)^2 - 4\kappa^2 x^2|) \\ &\quad + 4l\kappa xy (\kappa^2 + x^2 + y^2 - |-\kappa^2 + x^2 + y^2|) \\ &\geq l(l+2)(\kappa^2 + x^2 + y^2)^2(\tilde{\kappa}^2 - \kappa^2), \end{aligned}$$

and so we always have $\tilde{g}(z; \delta, l) > 0$ for the evanescent modes $\tilde{k} > k$ too. Together this shows that $R_{1d}^H(\tilde{k}) < 1$ for all evanescent modes. Note that, for the remaining modes $\tilde{k} \leq k$, it is possible that $R_{1d}^H(\tilde{k}) \geq 1$ for some choices of problem parameters.

We now refine the above bounds. In order to do so we make use of the identities $4x^2 y^2 = \kappa^2 s^2$ and $x^2 + y^2 = \sqrt{(\tilde{\kappa}^2 - \kappa^2)^2 + \kappa^2 s^2}$ which arise since (by considering both real and imaginary parts of $z^2 = (x + iy)^2 = i\kappa s + \tilde{\kappa}^2 - \kappa^2$) we have that

$$(4.5) \quad 2x^2 = \sqrt{(\tilde{\kappa}^2 - \kappa^2)^2 + \kappa^2 s^2} + \tilde{\kappa}^2 - \kappa^2, \quad 2y^2 = \sqrt{(\tilde{\kappa}^2 - \kappa^2)^2 + \kappa^2 s^2} - \tilde{\kappa}^2 + \kappa^2.$$

Now, if we make use of the substitution $\kappa^2 + x^2 = \tilde{\kappa}^2 + y^2$ for the terms involving hyperbolic functions and the substitution $\kappa^2 - y^2 = \tilde{\kappa}^2 - x^2$ for the terms involving trigonometric functions, we obtain the following:

$$\begin{aligned} \tilde{g}_{\pm}(z; \delta, l) &> [(\tilde{\kappa}^2 + 2y^2)x + 2\kappa y] lx - |(\tilde{\kappa}^2 - 2x^2)y - 2\kappa x| ly \\ &\geq l(x^2(\tilde{\kappa}^2 + 2y^2) - y^2|\tilde{\kappa}^2 - 2x^2|) \\ &= \begin{cases} l\tilde{\kappa}^2(x^2 + y^2) & \text{if } \tilde{\kappa}^2 \leq 2x^2, \\ l(4x^2 y^2 + \tilde{\kappa}^2(\tilde{\kappa}^2 - \kappa^2)) & \text{if } \tilde{\kappa}^2 > 2x^2, \end{cases} \\ &= \begin{cases} l\tilde{\kappa}^2 \sqrt{(\tilde{\kappa}^2 - \kappa^2)^2 + \kappa^2 s^2} & \text{if } \tilde{\kappa}^2 \leq 2x^2, \\ l(\tilde{\kappa}^4 + \kappa^2(s^2 - \tilde{\kappa}^2)) & \text{if } \tilde{\kappa}^2 > 2x^2, \end{cases} \end{aligned}$$

and

$$\begin{aligned} \tilde{g}(z; \delta, l) &> l(l+2) (x^2(\tilde{\kappa}^2 + 2y^2)^2 - y^2(\tilde{\kappa}^2 - 2x^2)^2) \\ &\quad + 4l\kappa xy (\tilde{\kappa}^2 + 2y^2 - |\tilde{\kappa}^2 - 2x^2|) \\ &= l(l+2) (\tilde{\kappa}^4(x^2 - y^2) + 4x^2 y^2(2\tilde{\kappa}^2 + y^2 - x^2)) \\ &\quad + 4l\kappa xy (\tilde{\kappa}^2 + 2y^2 - |\tilde{\kappa}^2 - 2x^2|) \\ &= \begin{cases} l(l+2) (\tilde{\kappa}^4(\tilde{\kappa}^2 - \kappa^2) + 4x^2 y^2(\tilde{\kappa}^2 + \kappa^2)) & \text{if } \tilde{\kappa}^2 \leq 2x^2, \\ \quad + 8l\kappa^3 xy & \\ l(l+2) (\tilde{\kappa}^4(\tilde{\kappa}^2 - \kappa^2) + 4x^2 y^2(\tilde{\kappa}^2 + \kappa^2)) & \text{if } \tilde{\kappa}^2 > 2x^2, \\ \quad + 8l\kappa xy(x^2 + y^2) & \end{cases} \\ &= \begin{cases} l(l+2) (\tilde{\kappa}^6 + \kappa^4 s^2 + \tilde{\kappa}^2 \kappa^2(s^2 - \tilde{\kappa}^2)) & \text{if } \tilde{\kappa}^2 \leq 2x^2, \\ \quad + 4l\kappa^4 s & \\ l(l+2) (\tilde{\kappa}^6 + \kappa^4 s^2 + \tilde{\kappa}^2 \kappa^2(s^2 - \tilde{\kappa}^2)) & \text{if } \tilde{\kappa}^2 > 2x^2, \\ \quad + 4l\kappa^2 s \sqrt{(\tilde{\kappa}^2 - \kappa^2)^2 + \kappa^2 s^2} & \end{cases} \end{aligned}$$

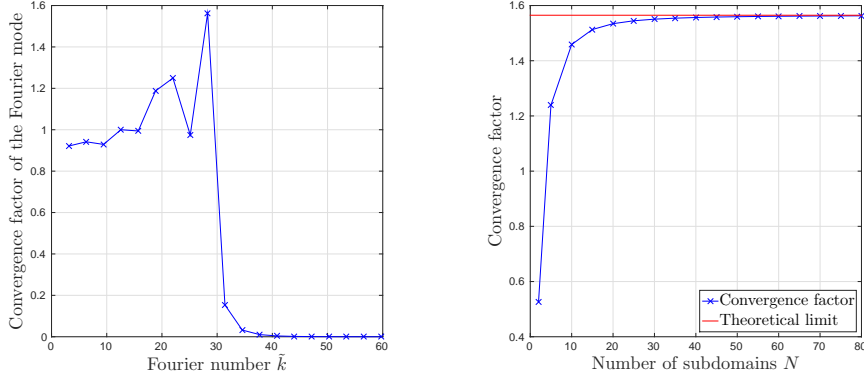


FIG. 4.1. The convergence factor of each Fourier mode for $N = 80$ (left) and the convergence factor of the full Schwarz algorithm for varying number of subdomains N (right) when $\sigma = 0.1$.

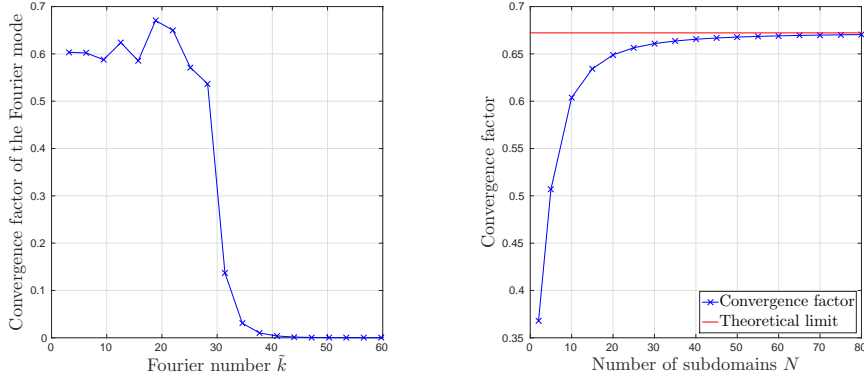


FIG. 4.2. The convergence factor of each Fourier mode for $N = 80$ (left) and the convergence factor of the full Schwarz algorithm for varying number of subdomains N (right) when $\sigma = 1$.

From the penultimate expression in each case we see that for evanescent modes $\tilde{k} > k$ (i.e. $\tilde{\kappa} > \kappa$) we always have $\tilde{g}_{\pm}(z; \delta, l) > 0$ and $\tilde{g}(z; \delta, l) > 0$. Furthermore, from the final expressions we see that all modes $\tilde{k} \leq \sigma$ (i.e. $\tilde{\kappa} \leq s$) also give the desired positivity. Thus we deduce that when $\sigma \geq k$ we have positivity for all modes \tilde{k} and hence $R_{2d}^H < 1$. We also remark that modes $\tilde{k} \leq k$ which are relatively close to k are identified as those giving the worst bounds, suggesting these are the most problematic modes for the algorithm.

If $\sigma < k$ we may still have positivity of $\tilde{g}_{\pm}(z; \delta, l)$ and $\tilde{g}(z; \delta, l)$ for all modes so long as x or lx is large enough so that the hyperbolic term, which is always positive, is larger than the magnitude of the trigonometric term in both (3.18b) and (3.20b). Using (4.5) and converting back to the original variables we have that

$$(4.6) \quad x = 2\delta \sqrt{\frac{1}{2} \left(\sqrt{(k^2 - \tilde{k}^2)^2 + \sigma^2 k^2} + \tilde{k}^2 - k^2 \right)},$$

while lx has an identical expression except with 2δ replaced by L . Thus we see that, between the parameters σ , δ and L , so long as they are sufficiently large we will have $\tilde{g}_{\pm}(z; \delta, l) > 0$ and $\tilde{g}(z; \delta, l) > 0$ for all modes \tilde{k} and thus $R_{2d}^H < 1$ as desired. \square

In order to verify this result, we compare numerically the spectral radius of the iteration matrix with the theoretical limit for different values of σ . We choose here $k = 30$, $L = 1$, $\hat{L} = 1$ and $\delta = L/10$. From Figures 4.1 and 4.2 we see that, as predicted, the Schwarz algorithm is not convergent for all Fourier modes when σ is small, but becomes convergent for σ sufficiently large. We also see that the algorithm converges well for the evanescent modes ($\tilde{k} > k$), as expected from our theory.

4.2. The transverse electric Maxwell's equations. We now apply the same ideas to the transverse electric Maxwell's equations with damping in the frequency domain. For an electric field $\mathbf{E} = (E_x, E_y)$, these equations are expressed as

$$(4.7) \quad \begin{aligned} \mathcal{L}\mathbf{E} &:= -k^2\mathbf{E} + \nabla \times (\nabla \times \mathbf{E}) + ik\sigma\mathbf{E} = \mathbf{0} \\ \Leftrightarrow \begin{cases} -k^2 E_x - \partial_{yy} E_x + \partial_{xy} E_y + ik\sigma E_x = 0, \\ -k^2 E_y - \partial_{xx} E_y + \partial_{xy} E_x + ik\sigma E_y = 0, \end{cases} \end{aligned}$$

for $(x, y) \in \Omega$. The boundary conditions on the top and bottom boundaries ($y = 0$ and $y = \hat{L}$) are perfect electric conductor (PEC) conditions, the equivalent of Dirichlet conditions for Maxwell's equations:

$$(4.8) \quad \mathbf{E} \times \mathbf{n} = \mathbf{0} \Leftrightarrow E_x = 0, \quad y = \{0, \hat{L}\}.$$

On the left and right boundaries ($x = a_1$ and $x = b_N$) we use impedance boundary conditions²:

$$(4.9) \quad \begin{aligned} (\nabla \times \mathbf{E} \times \mathbf{n}) \times \mathbf{n} + ik\mathbf{E} \times \mathbf{n} &= \mathbf{g} \\ \Leftrightarrow \begin{cases} \mathcal{B}_l \mathbf{E} := (-\partial_x + ik)E_y + \partial_y E_x = g_1, & x = a_1, \\ \mathcal{B}_r \mathbf{E} := (\partial_x + ik)E_y - \partial_y E_x = -g_2, & x = b_N. \end{cases} \end{aligned}$$

The same conditions will be used at the interfaces between subdomains, akin to the classical algorithm defined in [5]. The Maxwell problem (4.7)–(4.9) constitutes a “two-dimensional wave-guide” model.

Let us denote by \mathbf{E}_j^n the approximation to the solution in subdomain j at iteration n . Starting from an initial guess \mathbf{E}_j^0 , we compute \mathbf{E}_j^n from the previous values \mathbf{E}_j^{n-1} by solving the following local boundary value problems

$$(4.10) \quad \begin{cases} \mathcal{L}\mathbf{E}_j^n = \mathbf{0}, & x \in \Omega_j, \\ \mathcal{B}_l \mathbf{E}_j^n = \mathcal{B}_l \mathbf{E}_{j-1}^{n-1}, & x = a_j, \\ \mathcal{B}_r \mathbf{E}_j^n = \mathcal{B}_r \mathbf{E}_{j+1}^{n-1}, & x = b_j, \\ E_{x,j}^n = 0, & y \in \{0, \hat{L}\}, \end{cases}$$

for the interior subdomains ($1 < j < N$), while for the first ($j = 1$) and last ($j = N$) subdomain we impose $\mathcal{B}_l \mathbf{E}_1^n = g_1$ when $x = a_1$ and $\mathcal{B}_r \mathbf{E}_N^n = -g_2$ when $x = b_N$. To study the convergence of the Schwarz algorithm we define the local error in each subdomain j at iteration n as $\mathbf{e}_j^n = \mathbf{E}|_{\Omega_j} - \mathbf{E}_j^n$. Note that these errors verify boundary value problems which are the homogeneous counterparts of (4.10).

Due to the PEC boundary conditions on the top and bottom boundaries of each rectangular subdomain we can use the following Fourier series ansatzes to compute

²Note that in rewriting the impedance conditions we can use the three-dimensional definition of the operators, i.e. $\mathbf{E} = (E_x, E_y, 0)$ and $\mathbf{n} = (1, 0, 0)$ for the right boundary and $\mathbf{n} = (-1, 0, 0)$ for the left boundary.

the local solutions of $\mathcal{L}e_j^n = 0$:

$$(4.11) \quad e_{x,j}^n = \sum_{m=1}^{\infty} v_j^n(x, \tilde{k}) \sin(\tilde{k}y), \quad e_{y,j}^n = \sum_{m=1}^{\infty} w_j^n(x, \tilde{k}) \cos(\tilde{k}y), \quad \tilde{k} = \frac{m\pi}{\hat{L}}, \quad m \in \mathbb{N}.$$

By plugging the expressions for $e_{x,j}^n$ and $e_{y,j}^n$ into $\mathcal{L}e_j^n = \mathbf{0}$, a simple computation shows that, for each Fourier number \tilde{k} , we have the general solutions

$$(4.12) \quad v_j^n(x, \tilde{k}) = -\alpha_j^n \frac{\tilde{k}}{\zeta} e^{-\zeta x} + \beta_j^n \frac{\tilde{k}}{\zeta} e^{\zeta x}, \quad w_j^n(x, \tilde{k}) = \alpha_j^n e^{-\zeta x} + \beta_j^n e^{\zeta x},$$

where $\zeta(\tilde{k}) = \sqrt{ik\sigma + \tilde{k}^2 - k^2}$. From these formulae we can see easily that

$$(4.13) \quad \partial_x v_j^n = \tilde{k} w_j^n, \quad \partial_x w_j^n = \frac{\zeta^2}{\tilde{k}} v_j^n.$$

In order to benefit again from the analysis in the one-dimensional case, we first prove the following result.

LEMMA 4.2 (Maxwell reduction). *For each Fourier number \tilde{k} , we have that both $v_j^n(x, \tilde{k})$ and $w_j^n(x, \tilde{k})$ are solutions of the following one-dimensional problem:*

$$(4.14) \quad \begin{cases} (ik\sigma + \tilde{k}^2 - k^2)u_j^n - \partial_{xx}u_j^n = 0, & x \in (a_j, b_j), \\ \mathcal{B}_{l,\sigma}u_j^n(x, \tilde{k}) = \mathcal{B}_{l,\sigma}u_{j-1}^{n-1}(x, \tilde{k}), & x = a_j, \\ \mathcal{B}_{r,\sigma}u_j^n(x, \tilde{k}) = \mathcal{B}_{r,\sigma}u_{j+1}^{n-1}(x, \tilde{k}), & x = b_j, \end{cases}$$

where $\mathcal{B}_{l,\sigma} = -\partial_x + ik + \sigma$ and $\mathcal{B}_{r,\sigma} = \partial_x + ik + \sigma$.

Proof. Let us notice first that, because of (4.13), we have

$$\partial_x e_{x,j}^n + \partial_y e_{y,j}^n = \sum_{m=1}^{\infty} \left(\partial_x v_j^n - \tilde{k} w_j^n \right) \sin(\tilde{k}y) = 0.$$

If we use this in the error equation $\mathcal{L}e_j^n = \mathbf{0}$ we obtain that both $v_j^n(x, \tilde{k})$ and $w_j^n(x, \tilde{k})$ satisfy, for each \tilde{k} , the one-dimensional equation $(ik\sigma + \tilde{k}^2 - k^2)u_j^n - \partial_{xx}u_j^n = 0$. Let us analyse now the boundary conditions. With the help of (4.13), we consider the right boundary and note that the left one can be treated similarly:

$$\begin{aligned} \mathcal{B}_r e_j^n &= (\partial_x + ik)e_{y,j}^n - \partial_y e_{x,j}^n = \sum_{m=1}^{\infty} \left((\partial_x + ik)w_j^n - \tilde{k}v_j^n \right) \cos(\tilde{k}y) \\ &= \sum_{m=1}^{\infty} \left(\frac{ik}{\tilde{k}} \partial_x v_j^n + \left(\frac{\zeta^2}{\tilde{k}} - \tilde{k} \right) v_j^n \right) \cos(\tilde{k}y) = \sum_{m=1}^{\infty} \frac{ik}{\tilde{k}} \mathcal{B}_{r,\sigma} v_j^n \cos(\tilde{k}y). \end{aligned}$$

Thus, imposing transfer of boundary data with $\mathcal{B}_r e_j^n$ is equivalent to that with $\mathcal{B}_{r,\sigma} v_j^n$, for each Fourier number \tilde{k} . \square

It is now clear that the analysis of the two-dimensional case can again be derived from the one-dimensional case. That is, the result from Lemma 3.1 applies here if we replace α with $ik + \sigma$ and with ζ being defined by (4.4). Let us denote the resulting iteration matrix, for each \tilde{k} , by $\mathcal{T}_{1d}^M(\tilde{k})$ and let $R_{1d}^M(\tilde{k}) := \lim_{N \rightarrow \infty} \rho(\mathcal{T}_{1d}^M(\tilde{k}))$ with $R_{2d}^M = \sup_{\tilde{k}} R_{1d}^M(\tilde{k})$. We can now state our main convergence result for the two-dimensional Maxwell problem.

THEOREM 4.3 (Convergence of the Schwarz algorithm for Maxwell in 2D). *For all $k > 0$, $\sigma > 0$, $\delta > 0$ and $L > 0$ we have that $R_{1d}^M(\tilde{k}) < 1$ for all evanescent modes $\tilde{k} > k$. Furthermore, under the assumption that between them σ , δ and L are sufficiently large we have that $R_{2d}^M < 1$. In particular, this is true when $\sigma \geq k$ for all $\delta > 0$ and $L > 0$. Therefore the convergence will ultimately be independent of the number of subdomains (we say that the Schwarz method will scale).*

Proof. By [Lemma 3.2](#) we see that it is enough to study the sign of $g_{\pm}(z; \delta, l)$ and $g(z; \delta, l)$. To assist, we use the scaled notation $\kappa = 2\delta k$, $\tilde{\kappa} = 2\delta \tilde{k}$ and $s = 2\delta\sigma$ akin to [\(3.13\)](#). We can see that if $\alpha = ik + \sigma$ then for $z := x + iy$ [\(3.16\)](#) becomes

$$\Re v = \frac{-\kappa^2 - s^2 + x^2 + y^2}{(\kappa + y)^2 + (s + x)^2}, \quad \Im v = \frac{2sy - 2\kappa x}{(\kappa + y)^2 + (s + x)^2}, \quad |v|^2 = \frac{(\kappa - y)^2 + (s - x)^2}{(\kappa + y)^2 + (s + x)^2},$$

where $|v|^2 < 1$. We can now simplify $g_{\pm}(z; \delta, l)$ in [\(3.14\)](#) using these formulae to give

$$(4.15a) \quad g_{\pm}(z; \delta, l) = \frac{4e^{x(l+1)}}{(\kappa + y)^2 + (s + x)^2} \tilde{g}_{\pm}(z; \delta, l)$$

$$(4.15b) \quad \begin{aligned} \tilde{g}_{\pm}(z; \delta, l) &= [(\kappa^2 + s^2 + x^2 + y^2) \sinh(x) + 2(\kappa y + sx) \cosh(x)] \sinh(lx) \\ &\quad \pm [(\kappa^2 + s^2 - x^2 - y^2) \sin(y) + 2(sy - \kappa x) \cos(y)] \sin(ly). \end{aligned}$$

Proceeding as before, using $\tilde{\kappa}^2 - \kappa^2 = x^2 - y^2$ and the bounds [\(3.19\)](#), we derive that

$$\tilde{g}_{\pm}(z; \delta, l) > l(\kappa^2 + s^2 + 2s + x^2 + y^2)(\tilde{\kappa}^2 - \kappa^2)$$

which is positive for all evanescent modes $\tilde{k} > k$. Similarly, simplifying $g(z; \delta, l)$ in [\(3.15\)](#) we find that

$$(4.16a) \quad g(z; \delta, l) = \frac{4e^{2x(l+1)}}{((\kappa + y)^2 + (s + x)^2)^2} \tilde{g}(z; \delta, l)$$

$$(4.16b) \quad \begin{aligned} \tilde{g}(z; \delta, l) &= [((\kappa^2 + s^2 + x^2 + y^2)^2 + 4(\kappa y + sx)^2) \sinh(x(l+2)) \\ &\quad + 4(\kappa y + sx)(\kappa^2 + s^2 + x^2 + y^2) \cosh(x(l+2))] \sinh(lx) \\ &\quad + [((-\kappa^2 - s^2 + x^2 + y^2)^2 - 4(\kappa x - sy)^2) \sin(y(l+2)) \\ &\quad + 4(\kappa x - sy)(-\kappa^2 - s^2 + x^2 + y^2) \cos(y(l+2))] \sin(ly), \end{aligned}$$

from which we can obtain the bound

$$\begin{aligned} \tilde{g}(z; \delta, l) &> l(l+2) ((\kappa^2 + s^2 + x^2 + y^2)^2 + 4s^2(x^2 + y^2) + 8\kappa sxy) (\tilde{\kappa}^2 - \kappa^2) \\ &\quad + 4ls (\kappa^2 + s^2 + x^2 + y^2) (\tilde{\kappa}^2 - \kappa^2). \end{aligned}$$

Again, this is positive for all evanescent modes and thus we deduce that $R_{1d}^M(\tilde{k}) < 1$ for all $\tilde{k} > k$.

We now refine these bounds, as in the proof of [Theorem 4.1](#) and using the same identities and substitutions. For $g_{\pm}(z; \delta, l)$ we first obtain

$$\tilde{g}_{\pm}(z; \delta, l) > l(x^2(s^2 + \tilde{\kappa}^2 + 2y^2) - y^2 |s^2 + \tilde{\kappa}^2 - 2x^2| + 2x(\kappa y + sx) - 2y|\kappa x - sy|),$$

and split into four cases based on the sign of each term we take the absolute value of. Consider first the case $s^2 + \tilde{\kappa}^2 \leq 2x^2$ and $\kappa x \leq sy$, then

$$\begin{aligned} \tilde{g}_{\pm}(z; \delta, l) &> l((s^2 + \tilde{\kappa}^2)(x^2 + y^2) + 4\kappa xy + 2s(x^2 - y^2)) \\ &= l\left((s^2 + \tilde{\kappa}^2)\sqrt{(\tilde{\kappa}^2 - \kappa^2)^2 + \kappa^2 s^2} + 2\tilde{\kappa}^2 s\right). \end{aligned}$$

Now consider the case $s^2 + \tilde{\kappa}^2 > 2x^2$ and $\kappa x > sy$ where we find that

$$\begin{aligned}\tilde{g}_\pm(z; \delta, l) &> l(4x^2y^2 + (s^2 + \tilde{\kappa}^2)(x^2 - y^2) + 2s(x^2 + y^2)) \\ &= l\left(\tilde{\kappa}^2(s^2 + \tilde{\kappa}^2 - \kappa^2) + 2s\sqrt{(\tilde{\kappa}^2 - \kappa^2)^2 + \kappa^2s^2}\right).\end{aligned}$$

The remaining cases follow as combinations of the previous two cases and we deduce, in the case $s^2 + \tilde{\kappa}^2 \leq 2x^2$ and $\kappa x > sy$, that

$$\tilde{g}_\pm(z; \delta, l) > l(s^2 + \tilde{\kappa}^2 + 2s)\sqrt{(\tilde{\kappa}^2 - \kappa^2)^2 + \kappa^2s^2},$$

while the case $s^2 + \tilde{\kappa}^2 > 2x^2$ and $\kappa x \leq sy$ gives

$$\tilde{g}_\pm(z; \delta, l) > l\tilde{\kappa}^2(s^2 + \tilde{\kappa}^2 - \kappa^2 + 2s).$$

Turning to $\tilde{g}(z; \delta, l)$, we first derive that

$$\begin{aligned}\tilde{g}(z; \delta, l) &> l(l+2)[x^2((s^2 + \tilde{\kappa}^2 + 2y^2)^2 + 4(\kappa y + sx)^2) \\ &\quad - y^2((s^2 + \tilde{\kappa}^2 - 2x^2)^2 + 4(\kappa x - sy)^2)] \\ &\quad + 4l(x(\kappa y + sx)(s^2 + \tilde{\kappa}^2 + 2y^2) - y|(\kappa x - sy)(s^2 + \tilde{\kappa}^2 - 2x^2)|),\end{aligned}$$

from which we see that we need to analyse just two sets of combined cases. First consider when both $s^2 + \tilde{\kappa}^2 \leq 2x^2$ and $\kappa x \leq sy$ or both $s^2 + \tilde{\kappa}^2 > 2x^2$ and $\kappa x > sy$, yielding

$$\begin{aligned}\tilde{g}(z; \delta, l) &> l(l+2)[(s^2 + \tilde{\kappa}^2)^2(x^2 - y^2) + 4x^2y^2(2s^2 + 2\tilde{\kappa}^2 + y^2 - x^2) \\ &\quad + 4s(x^2 + y^2)(2\kappa xy + s(x^2 - y^2))] + 4l(x^2 + y^2)(2\kappa xy + s(s^2 + \tilde{\kappa}^2)) \\ &= l(l+2)\left[\kappa^2s^2(s^2 + \kappa^2) + \tilde{\kappa}^2(s^2 + \tilde{\kappa}^2)(s^2 + \tilde{\kappa}^2 - \kappa^2)\right. \\ &\quad \left.+ 4\tilde{\kappa}^2s^2\sqrt{(\tilde{\kappa}^2 - \kappa^2)^2 + \kappa^2s^2}\right] + 4ls(s^2 + \tilde{\kappa}^2 + \kappa^2)\sqrt{(\tilde{\kappa}^2 - \kappa^2)^2 + \kappa^2s^2}.\end{aligned}$$

On the other hand, in the second set of cases when both $s^2 + \tilde{\kappa}^2 \leq 2x^2$ and $\kappa x > sy$ or both $s^2 + \tilde{\kappa}^2 > 2x^2$ and $\kappa x \leq sy$ we have

$$\begin{aligned}\tilde{g}(z; \delta, l) &> l(l+2)[(s^2 + \tilde{\kappa}^2)^2(x^2 - y^2) + 4x^2y^2(2s^2 + 2\tilde{\kappa}^2 + y^2 - x^2) \\ &\quad + 4s(x^2 + y^2)(2\kappa xy + s(x^2 - y^2))] \\ &\quad + 4l(2\kappa xy(s^2 + \tilde{\kappa}^2 + y^2 - x^2) + s(4x^2y^2 + (s^2 + \tilde{\kappa}^2)(x^2 - y^2))) \\ &= l(l+2)\left[\kappa^2s^2(s^2 + \kappa^2) + \tilde{\kappa}^2(s^2 + \tilde{\kappa}^2)(s^2 + \tilde{\kappa}^2 - \kappa^2)\right. \\ &\quad \left.+ 4\tilde{\kappa}^2s^2\sqrt{(\tilde{\kappa}^2 - \kappa^2)^2 + \kappa^2s^2}\right] + 4ls(\kappa^2(s^2 + \kappa^2) + \tilde{\kappa}^2(s^2 + \tilde{\kappa}^2 - \kappa^2)).\end{aligned}$$

Summarising, we see that all cases give $\tilde{g}_\pm(z; \delta, l) > 0$ and $\tilde{g}(z; \delta, l) > 0$ for all modes \tilde{k} satisfying $\tilde{k}^2 \geq k^2 - \sigma^2$ (i.e. $\tilde{\kappa}^2 \geq \kappa^2 - s^2$). From this we can deduce that when $\sigma \geq k$ we have positivity for all modes \tilde{k} and hence $R_{2d}^M < 1$. Note that $\sigma \geq k$ is far from a necessary requirement and it is clear that there is some slack in these bounds. We also remark from this analysis that modes $\tilde{k} \leq \sqrt{k^2 - \sigma^2}$ which are relatively close to $\sqrt{k^2 - \sigma^2}$ yield the poorest bounds, suggesting they are the most problematic for the algorithm. Indeed, we may have $R_{1d}^M(\tilde{k}) \geq 1$ when $\tilde{k} \leq \sqrt{k^2 - \sigma^2}$ for some choices of problem parameters. However, as in [Theorem 4.3](#) we can force positivity of $\tilde{g}_\pm(z; \delta, l)$ and $\tilde{g}(z; \delta, l)$ for all modes so long as x or lx is large enough. Since x and lx take the same expressions as in [Theorem 4.3](#) we can similarly deduce that, so long as the parameters σ , δ and L between them are sufficiently large, we will have $\tilde{g}_\pm(z; \delta, l) > 0$ and $\tilde{g}(z; \delta, l) > 0$ for all modes \tilde{k} and thus the required conclusion that $R_{2d}^M < 1$. \square

5. Numerical simulations on the discretised equation. Although extensive numerical results are beyond the scope of this paper, in the following we will show some simulations which confirm our theory within the more practical setting of using an iterative Krylov method to accelerate convergence, with the Schwarz method being used as a preconditioner. We focus here on the two-dimensional Helmholtz equation, as described in Section 4, where a (horizontal) plane wave is incoming from the left boundary and homogeneous Dirichlet boundary conditions are imposed on the top and bottom boundaries, giving a wave-guide problem. A second test case we consider is the propagation of such a wave in free space (i.e. when impedance boundary conditions are imposed on the whole boundary). While not covered by our theory, we will nonetheless observe similar conclusions, illustrating that the results apply more widely than within the restrictions of our theoretical assumptions. In our simulations, each subdomain is a unit square split uniformly with a fixed number of grid points in each direction. New subdomains are added on the right so that, with N subdomains, the whole domain is $\Omega = (0, N) \times (0, 1)$.

To discretise we use a uniform square grid in each direction and triangulate with alternating diagonals to form P1 elements. As we increase k we increase the number of grid points proportional to $k^{3/2}$ in order to ameliorate the pollution effect [1]. We use an overlap of size $2h$, with h being the mesh size. All computations are performed using FreeFem (<http://freefem.org/>), in particular using the `ffddm` framework. We solve the discretised problem using GMRES where the Schwarz method with Robin conditions is used as a preconditioner. In particular, we use right-preconditioned GMRES and terminate when a relative residual tolerance of 10^{-6} is reached. The construction of the domain decomposition preconditioner is described in detail in [2, 9]. The one-level ORAS preconditioner is $\mathbf{M}^{-1} = \sum_{i=1}^N \mathbf{R}_i^T \mathbf{D}_i \mathbf{A}_i^{-1} \mathbf{R}_i$ where $\{\mathbf{R}_i\}_{1 \leq i \leq N}$ are the Boolean restriction matrices from the global to the local finite element spaces and $\{\mathbf{D}_i\}_{1 \leq i \leq N}$ are local diagonal matrices representing the partition of unity. The key ingredient of the ORAS method is that the local matrices $\{\mathbf{A}_i\}_{1 \leq i \leq N}$ incorporate more efficient Robin transmission conditions.

Note that, unlike in [18] where the emphasis is placed on the independence of the one-level method to the wave number, we focus here on the scalability aspect, i.e. the independence of the one-level method with respect to the number of subdomains N as soon as the absorption parameter $k\sigma$ is positive. We will observe that, beyond a sufficiently large value of N , the iteration count does not increase further, though in general this value will depend on the parameters of the problem, namely the wave number and absorption as well as the overlap and subdomain size. As a side effect, when the absorption is sufficiently large, i.e. of order k , wave number independence is also achieved.

In Table 5.1 we detail the GMRES iteration count for an increasing number of subdomains N and different values of k for the wave-guide problem and the wave propagation in free space problem. We set the conductivity parameter as $\sigma = 1$ (giving an absorption parameter k). We see that, after an initial increase, the iteration counts become independent of the number of subdomains and also independent of the wave number, which is consistent with the results obtained in [18] where the absorption parameter for optimal convergence is of order k . Another possible explanation of this is that when the absorption parameter increases, the waves are damped and their amplitude will decrease with the distance to the boundary on which the excitation is imposed. Hence, when additional subdomains are added, the solution will not vary much in these subdomains.

TABLE 5.1

Preconditioned GMRES iteration counts for varying wave number k and number of subdomains N when $\sigma = 1$.

k/N	Wave-guide problem								Free space problem							
	8	16	24	32	40	48	56	64	8	16	24	32	40	48	56	64
20	19	22	25	30	30	30	30	30	19	21	25	25	25	25	25	25
40	18	21	24	29	29	29	29	29	17	19	24	25	25	25	25	25
60	19	21	24	29	29	29	29	29	16	19	24	25	25	25	25	25
80	19	21	24	28	28	28	28	28	16	18	24	25	25	25	25	25
100	19	21	24	28	28	28	28	28	16	18	24	25	25	25	25	24

6. Conclusions. In this work we have analysed a purely iterative version of the Schwarz domain decomposition algorithm, in the limiting case of many subdomains, at the continuous level for the one-dimensional and two-dimensional Helmholtz and Maxwell's equations with absorption. The key mathematical tool which facilitated this study is the limiting spectrum of a sequence of block Toeplitz matrices having a particular structure, for which we proved a new result in the non-Hermitian case. The algorithm is convergent in the one-dimensional case as soon as we have absorption and, for sufficiently many subdomains N , its convergence factor becomes independent of the number of subdomains, meaning the algorithm is also scalable. In practice, this is achieved for relatively small N . In the two-dimensional case these conclusions remain true for the evanescent modes of the error (i.e. $\tilde{k} > k$) or when, between them, σ , δ and L are sufficiently large. In particular, we proved that the stationary iteration will always converge when $\sigma \geq k$, giving an absorption parameter k^2 . The concept of the limiting spectrum proved to be a very elegant mathematical tool and can be used, for example, in constructing more sophisticated transmission conditions, to analyse the algorithm at the discrete level, or to design improved preconditioners.

REFERENCES

- [1] I. M. Babuška and S. A. Sauter. Is the pollution effect of the FEM avoidable for the Helmholtz equation considering high wave numbers? *SIAM J. Numer. Anal.*, 34(6):2392–2423, 1997.
- [2] M. Bonazzoli, V. Dolean, I. G. Graham, E. A. Spence, and P.-H. Tournier. Domain decomposition preconditioning for the high-frequency time-harmonic Maxwell equations with absorption. *Math. Comp.*, 88:2559–2604, 2019.
- [3] R. Brunet, V. Dolean, and M. J. Gander. Natural domain decomposition algorithms for the solution of time-harmonic elastic waves. *arXiv e-prints*, arXiv:1904.12158, 2019.
- [4] F. Chaouqui, G. Ciaramella, M. J. Gander, and T. Vanzan. On the scalability of classical one-level domain-decomposition methods. *Vietnam J. Math.*, 46:1053–1088, 2018.
- [5] B. Després, P. Joly, and J. E. Roberts. A domain decomposition method for the harmonic Maxwell equations. In *Iterative methods in linear algebra (Brussels, 1991)*, pages 475–484. North-Holland, Amsterdam, 1992.
- [6] V. Dolean, M. J. Gander, and L. Gerardo-Giorda. Optimized Schwarz methods for Maxwell's equations. *SIAM J. Sci. Comput.*, 31(3):2193–2213, 2009.
- [7] V. Dolean, M. J. Gander, S. Lanteri, J.-F. Lee, and Z. Peng. Effective transmission conditions for domain decomposition methods applied to the time-harmonic curl–curl Maxwell's equations. *J. Comput. Phys.*, 280:232–247, 2015.
- [8] V. Dolean, P. Jolivet, and F. Nataf. *An Introduction to Domain Decomposition Methods: Algorithms, Theory, and Parallel Implementation*. SIAM, Philadelphia, 2015.
- [9] V. Dolean, P. Jolivet, P.-H. Tournier, and S. Operto. Iterative frequency-domain seismic wave solvers based on multi-level domain-decomposition preconditioners. In *82th Annual EAGE Meeting (Amsterdam)*, 2020. arXiv:2004.06309.
- [10] V. Dolean, S. Lanteri, and R. Perrussel. A domain decomposition method for solving the three-dimensional time-harmonic Maxwell equations discretized by discontinuous Galerkin methods. *J. Comput. Phys.*, 227(3):2044–2072, 2008.

- [11] M. Donatelli, M. Neytcheva, and S. Serra-Capizzano. Canonical eigenvalue distribution of multilevel block Toeplitz sequences with non-Hermitian symbols. In *Spectral Theory, Mathematical System Theory, Evolution Equations, Differential and Difference Equations*, pages 269–291. Springer, 2012.
- [12] M. El Bouajaji, V. Dolean, M. J. Gander, and S. Lanteri. Optimized Schwarz methods for the time-harmonic Maxwell equations with damping. *SIAM J. Sci. Comput.*, 34(4):A2048–A2071, 2012.
- [13] O. G. Ernst and M. J. Gander. Why it is difficult to solve Helmholtz problems with classical iterative methods. In I. Graham, T. Hou, O. Lakkis, and R. Scheichl, editors, *Numerical Analysis of Multiscale Problems*, pages 325–363. Springer, Berlin, 2012.
- [14] M. J. Gander, L. Halpern, and F. Magoulès. An optimized Schwarz method with two-sided Robin transmission conditions for the Helmholtz equation. *Internat. J. Numer. Methods Fluids*, 55(2):163–175, 2007.
- [15] M. J. Gander and H. Zhang. A class of iterative solvers for the Helmholtz equation: Factorizations, sweeping preconditioners, source transfer, single layer potentials, polarized traces, and optimized Schwarz methods. *SIAM Rev.*, 61(1):3–76, 2019.
- [16] S. Gong, I. G. Graham, and E. A. Spence. Domain decomposition preconditioners for high-order discretisations of the heterogeneous Helmholtz equation. *arXiv e-prints*, arXiv:2004.03996, 2020.
- [17] I. G. Graham, E. A. Spence, and E. Vainikko. Recent results on domain decomposition preconditioning for the high-frequency helmholtz equation using absorption. In D. Lahaye, J. Tang, and K. Vuik, editors, *Modern Solvers for Helmholtz Problems*, Geosystems Mathematics, pages 3–26. Birkhäuser, Cham, 2017.
- [18] I. G. Graham, E. A. Spence, and J. Zou. Domain decomposition with local impedance conditions for the Helmholtz equation. *arXiv e-prints*, arXiv:1806.03731, 2018.
- [19] I. I. Hirschman. The spectra of certain Toeplitz matrices. *Illinois J. Math.*, 11:145–159, 1967.
- [20] V. Mattesi, M. Darbas, and C. Geuzaine. A high-order absorbing boundary condition for 2D time-harmonic elastodynamic scattering problems. *Comput. Math. Appl.*, 77(6):1703–1721, 2019.
- [21] A. Sandryhaila and J. M. F. Moura. Eigendecomposition of block tridiagonal matrices. *arXiv e-prints*, arXiv:1306.0217, 2013.
- [22] P. Schmidt and F. Spitzer. The Toeplitz matrices of an arbitrary Laurent polynomial. *Math. Scand.*, 8:15–38, 1960.
- [23] P. Tilli. A note on the spectral distribution of Toeplitz matrices. *Linear Multilinear Algebra*, 45(2–3):147–159, 1998.
- [24] M. Tismenetsky. Determinant of block-Toeplitz band matrices. *Linear Algebra Appl.*, 85:165–184, 1987.
- [25] K. Tran. Connections between discriminants and the root distribution of polynomials with rational generating function. *J. Math. Anal. Appl.*, 410(1):330 – 340, 2014.
- [26] H. Widom. Asymptotic behavior of block Toeplitz matrices and determinants. *Adv. Math.*, 13:284–322, 1974.